EFFECTS OF ACTIVATOR POWDERS ON HYBRID BINDERS BASED ON VOLCANIC ASH AND PORTLAND CLINKER BASED CEMENT.

H.K Havanjana Lanka Fernando

A thesis submitted in fulfillment of the requirements

for the Degree of Master of Engineering

Main supervisor: Dr Zhiyuan (Arthur) Fang

Co-supervisors: Dr. Krishanu Roy, Dr. Kim de Graaf, and Kushal Ghosh

School of Engineering

The University of Waikato

New Zealand

THE UNIVERSITY OF
WAIKATO
Te Whare Wānanga o Waikato

2025

ABSTRACT

Concrete remains the most widely used construction material worldwide. However, the high energy consumption and CO_2 emissions associated with Portland cement production have driven the search for more sustainable alternatives. Volcanic ash (VA), a naturally occurring pozzolan found in abundance in regions such as Tauranga, New Zealand, presents promising potential as a partial replacement for cement.

This thesis investigates the performance of value-added products from the Takitimu North Link (TNL) site, using chemical activation with sodium sulphate (Na_2SO_4) and calcium hydroxide ($Ca(OH)_2$) in hybrid binder systems. A central composite experimental design was employed to systematically vary the VA content and activator dosages.

Mortar mixes with 25%, 50%, 75%, and 100% VA replacement were tested (Series A), with particular focus on the 25% blend. This composition underwent further testing with varying activator dosages to determine the optimal $Na_2SO_4/Ca(OH)_2$ (NS/CH) ratio (Series B). Compressive strength tests were conducted at 7, 28, and 90 days to assess mechanical performance.

Additionally, microstructural characterization techniques including scanning electron microscopy (SEM), X-ray diffraction (XRD), Fourier-transform infrared spectroscopy (FTIR), and thermogravimetric analysis (TGA) were used to identify hydration products and evaluate binder densification.

The results showed that a 25% replacement of Portland cement with VA, activated with 14% Na_2SO_4 at an NS/CH ratio of 1, delivered optimal compressive strength and microstructural development. While higher replacement levels generally reduced early-age strength due to weaker pozzolanic activity, appropriate activator dosages improved long-term performance significantly.

Overall, the study demonstrates that chemically activated volcanic ash can substantially improve the sustainability profile of concrete by reducing Portland cement usage and its environmental impacts. The use of optimized hybrid binders incorporating volcanic ash offers a viable solution for developing sustainable, resilient, and cost-effective construction materials in New Zealand and other volcanic regions worldwide.

PREFACE

This thesis is presented to the University of Waikato, New Zealand, in completion of the criteria for obtaining the Master's Degree in Civil Engineering. The research presented in this thesis has not been formerly submitted for a degree or diploma at any other institution of higher learning. To the best of my knowledge and belief, the thesis does not include any significant material that has been published or authored by someone else, unless appropriate acknowledgment is provided.

ACKNOWLEDGEMENTS

First and foremost, I would like to convey my heartfelt gratitude to my chief supervisor, Dr. Zhiyuan (Arthur) Fang, for his guidance, support, and encouragement during the duration of this research. His guidance and mentorship have played a vital role in developing this thesis.

I would also like to express my sincere gratitude to my co-supervisors, Dr. Krishanu Roy, Kim de Graaf and Kushal Ghosh for their constant support and positive criticism, which added immense value to the width and depth of my research. My special thanks also go to Balasubramanian for his ongoing support and motivation throughout the experimental and writing stages.

Special reference must be made to my good friend, Darshi Egodage, whose support and positivity throughout the year added greatly towards my academic achievement.

I also acknowledge the University of Waikato, School of Engineering, and all technical professionals and laboratory technicians for offering the facilities and support to conduct my research.

Lastly, I want to thank my family, particularly my husband for their unconditional love, patience, and support. They had faith in me, and I was able to continue and finish my Master degree.

NOTATIONS

VA- General Volcanic Ash

RVA – Rhyolitic Volcanic Ash (the sample tested)

Control sample (mix) - this refers to a mix with no replacement of cement

OPC – Ordinary Portland Cement

NS – Sodium Sulphate

CH – Calcium Hydroxide

CS – Compressive strength

% - Percentage

NS/CH – Mass ratio of Sodium Sulfate to Calcium Hydroxide in the mix

SEM - Scanning Electron Microscopy (image of surface morphology)

BSE - Back-Scattered Electron imaging (grayscale contrast by atomic number)

EDS - Energy-Dispersive X ray Spectroscopy (elemental mapping in SEM)

XRD – X-ray Diffraction (crystalline phase identification)

FTIR - Fourier Transform Infrared Spectroscopy (molecular and bond identification)

TGA/DTG - Thermogravimetric Analysis / Derivative Thermogravimetry (mass change on heating)

C-S-H - Calcium Silicate Hydrate (primary binding gel in hydrated cement)

C-A-S-H – Calcium Aluminosilicate Hydrate (AL enriched binding gel from pozzolanic reaction)

TABLE OF CONTENTS

LIST OF FIGURES

LIST OF TABLES

CHAPTER 1. INTRODUCTION

1.1 Introduction

Concrete is the fundamental material of contemporary infrastructure and the most widespread construction material globally [1]. The primary ingredients - cement, sand, aggregates, and water are essential to its function; yet their production and extraction have significant environmental effects. Cement manufacturing is a paramount source of global carbon dioxide (CO_2) emissions, mainly owing to the calcination of limestone and the intensive energy requirements of clinker production [1, 2]. The environmental issues of concrete manufacturing, along with natural resource depletion and the increased demand for sustainable construction methods, have motivated researchers to find substitute materials and new techniques to minimize concrete's carbon footprint.

Partial replacement of cement with supplementary cementitious materials (SCMs) is a promising approach, as it can enhance the sustainability of concrete without compromising its mechanical and durability properties [3]. One such material is volcanic ash, a naturally occurring, pozzolanic material with high silica and alumina content [4]. When blended with Portland cement, volcanic ash responds with calcium hydroxide ($Ca(OH)_2$) [5] on hydration in a reaction to form additional calcium silicate hydrate (C-S-H) gels [6], the primary binding phase for strength and durability of cementitious systems. This reaction not only improves the performance of concrete but also reduces the overall clinker factor, thereby reducing CO_2 emissions from cement production.

The utilization of volcanic ash in hybrid binders in an effective way requires chemical activation to stimulate its reactivity and improve the mechanical performance of the product [7]. Chemical activators like sodium sulfate (Na_2SO_4) and calcium hydroxide ($Ca(OH)_2$) [8] play a key role in promoting the pozzolanic reaction and microstructural characteristics of the volcanic ash binder. Sodium sulfate, for example, can increase early-age strength by facilitating the development of ettringite, whereas calcium hydroxide supplies the essential alkalinity to support the pozzolanic reaction over a prolonged period.

This study investigates the influence of sodium sulfate and calcium hydroxide as activating agents on hybrid binders composed of volcanic ash and Portland clinker-based cement. Through systematic alteration of the content of volcanic ash and the activating agents, this research seeks to enhance both the mechanical and microstructural performance of the hybrid binder and lower its environmental footprint. The outcome of this study is anticipated to play a role in the development of sustainable construction materials using locally available materials, like volcanic ash, with a view to limiting the

use of traditional cement and advancing the circular economy ideals. In the end, this study aspires to fill the gap between performance and sustainability, offering a realistic way forward to greener and more durable infrastructure.

1.2 Aims and Objectives

The primary objective of the study is to evaluate the suitability of volcanic Ash (VA), sourced from the Takitimu North Link (TNL) project in Tauranga, North Island, New Zealand, as a supplementary material in hybrid cementitious systems. The aim of the study is to investigate the effect of VA and solid activator powders on the physical, mechanical, and microstructural properties of mortar mixtures incorporating Portland clinker-based cement. Sodium sulphate and calcium hydroxide are used as chemical activators to increase the reactivity of the VA and to stimulate the formation of new cementitious phases.

The detailed objectives are as follows:

- Characterize the physical and chemical properties of sand, cement, and volcanic ash.
- Assess the normal consistency, initial and final setting times of cementitious pastes incorporating VA and activator powders.
- Determine the workability of fresh mortar mixtures containing varying proportions of VA and fixed or variable dosages of sodium sulphate and calcium hydroxide.
- Evaluate the compressive strength development of VA-based hybrid mortar mixtures at different curing ages.
- Examine the microstructural characteristics and hydration products with scanning electron microscopy (SEM), energy-dispersive X ray spectroscopy (EDS), and X ray diffraction (XRD).
- Analyse molecular bond formations using Fourier transform infrared spectroscopy (FTIR).
- Assess the thermal stability and decomposition behaviour of hydration products through TGA and DTG.

1.3 Research Gap

Although volcanic ash has been researched extensively as an adjunct cementitious material, certain research gaps still persist. Specifically, New Zealand volcanic ash, particularly Hamilton Ash from Tauranga, has never before been researched in hybrid binder systems due to its distinctive chemical composition. Moreover, most prior research with volcanic ash primarily uses liquid activators; however, this present study advocates for solid-state activators (Na_2SO_4 and $Ca(OH)_2$) as a safer and

more practical alternative. The application of statistical optimization in mix design is also limited; this study utilizes response surface methodology to comprehensively assess key variables. Extensive microstructural investigations using SEM, XRD, FTIR, and TGA are seldom reported in the existing literature. Finally, environmentally friendly reuse of locally sourced volcanic ash to enable circular economy practices in New Zealand's construction industry is a new and inadequately explored approach covered in this study.

1.4 Scope of work

The research aims to evaluate how varying quantities of volcanic ash (25%, 50%, 75%, 100% by mass) and activator dosage affect the mechanical and microstructural properties of the resulting binders.

The scope includes:

- Designing and preparing mortar blends with varying proportions of volcanic ash (as partial replacement for cement) along with consistent or adjustable amounts of sodium sulfate (NS % from VA - 6,8,10,12,14) and calcium hydroxide as solid-state activators (NS/CH = 0.25, 0.5, 0.75, 1, 1.25).
- Assessing the properties of the mixtures in their fresh state, such as consistency and workability, using standard flow tests.
- Performing compressive strength tests at multiple curing ages (7, 14, and 28 days) to analyse mechanical performance and identify optimal mix compositions.
- Performing detailed microstructural characterization on selected mixes using SEM for morphology (BSE and SE on resin based polished and non-polished powder samples), EDS for elemental analysis, XRD (angle 5° to 90°) for phase identification, and FTIR for chemical bonding analysis.
- Evaluating the thermal stability of hydration products and decomposition behaviour using TGA and DTG techniques (temperature 30-800 °C).

CHAPTER 2. LITERATURE REVIEW

2.1 Introduction

The construction industry is one of the world's biggest consumers of resources and significantly contributes to environmental effects, particularly through the production of concrete [1, 9]. The major component of concrete is Ordinary Portland Cement (OPC)**,** which requires large amounts of energy to produce and a significant source of worldwide carbon dioxide (CO2) emissions [9]. On the basis of increasing environmental concerns and a rising demand for sustainable construction practice, it is necessary to investigate alternative binder systems. New Zealand has extensive deposits of volcanic ash, a result of its rich history of volcanic activity. These deposits come in various forms, including Taupo Pumice found in areas like Horotiu [10], Rotoehu Ash in Tauranga [11], Hamilton Ash in Waikato District [12] and Volcanic Pumice (VP) sourced from Mangakino and the Kaimai region. Kaimai pumice has been commercially used in some hydro-electric projects in the Waikato region [13]. In addition to volcanic ash, other industrial by-products such as fly ash and slag are also being explored for their potential use as supplementary cementitious materials (SCMs) in concrete mixes.

This literature review will outline advancements in green concrete production via cement substitution and particularly deals with the use of volcanic ash (VA) and its activation via either chemical or hybrid binder systems consisting of VA and OPC

2.2 Cement, Production and Environmental Impact

2.2.1 Ordinary Portland Cement and Production

OPC is the second most widely used substance after water and forms the basis of mortar and concrete [1, 14]. The ongoing growth of the constructed environment to meet the demands of an expanding global population continues to increase the need for cement-based materials [1, 14, 15]. In numerous nations OPC, also known as ordinary Portland cement (PC), is the widely utilized binder for producing concrete [14, 16, 17]. The term 'cement' frequently denotes Portland cement in particular [10]. Manufacturing OPC involves cement clinker production, which is the active binding ingredient of concrete [18], which is highly energy and fossil fuel consuming process [16, 19]. A considerable amount of energy is necessary in the manufacturing of OPC [4]. The production of clinker requires roughly 3.4 GJ of energy per ton and includes the decarbonization of limestone, leading to considerable CO_2 emissions [10, 15, 17, 20]. The production alone of OPC accounts for a large percentage of

anthropogenic CO_2 emissions emitted worldwide, an estimated 5% to 8% [9, 15, 21-26], and its lifecycle share is estimated to be as high as 10-17% of total emissions [16, 17, 22].

2.2.2 Environmental Concerns

The manufacturing and overuse of OPC poses a major environmental issue owing to resource depletion and energy expenditure [9]. The cement production is a source of greenhouse gas (GHG) emissions, primarily CO_2 from limestone calcination and kiln fuel combustion [15-17, 25]. Greenhouse gas emissions are known to accelerate climate change and a reduction in this effect necessitates a shift to more eco-efficient alternatives [14, 21, 25, 27-30]. Added to this, the mining of raw materials for cement manufacture drains natural resources, and hence there is a need to use eco efficient alternatives [1, 9, 31].

In 2020, global cement production hit 4.1 billion tons [17], annual production generally lies between and 2.8 to 4.1 billion tons [16, 26]. In 2016, cement production yielded 1.46 ± 0.19 Gt of CO_2 [26]. For each kilogram of Portland cement manufactured, a considerable quantity of carbon dioxide (CO_2) is released into the atmosphere [19]. It has been calculated that nearly one ton of CO_2 is released for every ton of Portland cement manufactured [15, 22, 32], with about 2/3 of these emissions arising from the thermal breakdown of calcium carbonate (limestone) and the remaining 1/3 coming from fuel combustion to reach the required temperatures for this process [20]. The extraction and processing of large quantities of raw materials for cement annually impact the environment [4], resulting in resource depletion and ecological harm [32]. Kiln combustion releases carbon dioxide, nitrogen oxide, water, oxygen, dust, sulphur dioxide, fluorides, carbon monoxide, chlorides, and trace amounts of organic chemicals, which harm ecosystems and raises environmental concerns [19]. Addressing the growing need for cement-based materials through conventional methods will result in an intolerable rise in CO_2 emissions [1] and irreversible environmental damage.

2.3 Role of Supplementary Cementitious/Pozzolanic Materials in Sustainable Construction

2.3.1 Definition and Types

One of the most important ways to minimize the environmental impact of concrete is the partial or complete replacement of OPC with supplementary cementitious materials (SCMs) [1, 17, 21, 23, 26, 33]. SCMs containing industrial waste products, natural minerals, and processed natural materials have hydraulic or pozzolanic behavior that improve hardened concrete properties [17, 19, 30, 34]. The use

of SCMs in cementitious materials saves embodied energy, decreases greenhouse gas emissions, conserves resources, and even reduces constructions costs, all leading to a more sustainable built environment [9, 16, 19, 21, 30].

A few typical SCMs include fly ash (FA), ground granulated blast furnace slag (GGBS), silica fume (SF) [34], and natural pozzolans such as VA [24, 31], and pumice [24]. Not only do these materials lower the demand for OPC, and thus lower CO_2 emissions and energy use [19, 21, 23], they can also enhance concrete durability, reduce permeability, enhance sulfate and chloride resistance, and mitigate alkali-silica reactions [19, 23, 30, 35, 36]. Further, the utilization of waste materials as SCMs is beneficial in mitigating waste disposal issues and promoting a circular economy [17, 19].

Pozzolanic materials consist of siliceous elements that, when finely ground and exposed to moisture, interact with calcium hydroxide produced from OPC hydration to create cement like compounds [19, 37]. Occasionally called mineral admixtures [19], these might not possess natural pozzolanic characteristics but acquire them when mixed with Portland cement [19].

Various kinds of pozzolanic substances have been considered in earlier research:

- Natural Pozzolans: These include VA [16, 17, 21, 24, 25, 37], VP [23], volcanic tuff (VT) [29], and other naturally occurring pozzolans found in different geological formations.
- Artificial/Industrial By-Product Pozzolans: This category consists of FA [17, 38], ground granulated blast furnace slag (GGBS) [39], silica fume (SF) [36], rice husk ash (RHA) [8, 40, 41], and calcined clay [33, 42].
- Processed Natural Materials: Certain natural pozzolans, such as VP, might be subjected to heat treatment or grinding to improve their pozzolanic performance [8, 38]. Activation techniques may involve mechanical, chemical, and sometimes thermal processes [8].

2.3.2 Benefits for Reducing Environmental Impact

The integration of pozzolanic elements in cement and concrete manufacturing provides substantial advantages in mitigating environmental impact:

- **Reduction of CO_2 Emissions**: research indicates that even a minor fraction of cement substitution with SCMs can greatly diminish the greenhouse effect [19]. For example, concrete containing VA has been linked to notably reduced GHG emissions in comparison to concrete made solely with OPC and various industrial SCMs [16]. Volcanic ash-limestone concrete (VLC) and volcanic ash

concrete (VC) have demonstrated a 25% reduction in greenhouse gas emissions when compared to standard concrete (NC) made with OPC [9].

- **Conservation of Natural Resources and Energy Savings**: Utilizing pozzolanic materials that are by products or abundant in nature, reduces the need for new limestone and lessens the energy required to manufacture clinker [4, 17, 37, 38]. The energy required for heat in clinker production is considerable [1, 2]. Replacing cement with pozzolans aids in energy conservation and environmental protection [3] .
- **Utilization of Waste Materials**: Incorporating waste by-products such as FA, GGBS, RHA, and specific volcanic materials into concrete alleviates waste disposal challenges and improves resource recycling by transforming non-renewable substances into more sustainable, partially renewable alternatives[8, 21, 23].
- **Lower Embodied Energy:** Natural pozzolans such as VA need less energy for extraction and processing than PC. Incorporating VA as a substitute for a part of OPC in concrete can consequently reduce the embodied energy of the concrete [21, 38, 43] . For example, research indicated an average reduction of 16% in EEC values when 40% of OPC was substituted with VA [21]. This means using this type of the material will decrease in initial embodied energy of structures.
- **Improved Durability**: Although it does not directly lessen environmental impacts, the increased durability of pozzolan-containing concrete (which includes better resistance to sulphate attacks, alkali-aggregate reactions, and chloride infiltration) can prolong the lifespan of structures, indirectly reducing the environmental strain linked to regular repairs and replacements [24, 35, 37, 44].

In general, utilizing pozzolanic materials to partially substitute for OPC or PC is an encouraging approach to lessen the environmental footprint of the construction sector, contributing to the development of more sustainable and environmentally friendly cement-based products [1, 16, 17, 35].

2.4 Use of Volcanic Ash in Cementitious Materials

2.4.1 Properties of Volcanic Ash

VA is identified as a natural pozzolan based on ASTM C618. Its chemical composition predominantly consists of oxides like SiO_2, Al_2O_3, CaO, Fe_2O_3, MgO, K_2O, and Na_2O is intricately linked to the chemistry of the originating magma [4, 43-45].

Particle Morphology

Volcanic ash refers to tiny particles of pyroclastic materials, usually less than 2mm in size and also ground or powdered volcanic scoria and slags [43]. The density of single particles can change considerably based on the type of pyroclastic material: pumice ranges from 700–1200 kg/m3, glass shards from 2350–2450 kg/m3, crystals from 2700–3300 kg/m3, and lithic particles from 2600–3200 kg/m3 [43, 45]. The bulk density also differs; for crushed particles smaller than 0.075mm, pumice has a density of 2.46 g/cm³, while scoria shows a density of 2.98 g/cm³ [43].

Volcanic ash is valued for its physical characteristics like fine particle size, angularity, fragility, colour, and chemical qualities [45, 46]. The size distribution of crucial for the successful alkaline activation of aluminosilicates [47]. Indeed, a finer VA (µm scale) can substitute for a greater amount of Portland cement, resulting in a denser pore structure and the creation of more C-S-H gels that enhance concrete strength [48, 49].

Chemical Composition

Table 1 presents a summary of the chemical composition of volcanic ashes derived through different research projects. In most instances, SiO_2 is the dominant oxide, typically ranging from 40 to 52 wt.% for basic lava like scoria and 63–75% for acidic lava like pumice [45].

Table 1 Chemical compositions of VA from various investigations

Origin and References	SiO_2	Al_2O_3	Fe_2O_3	CaO	MgO	Na_2O	K_2O	LOI
	(wt. %)							
Cameroon [47]	40.1	16.3	13.5	6.3	5.3	0.8	0.5	11.1
	45.8	13.8	13.5	11.8	8.4	3.2	1.5	0.1
	45.3	12.4	12.9	13.1	9.9	2.4	1.3	0.2
	46.1	14	13.1	10.7	7	2.7	1.4	1.5
	45.5	12.6	13.3	13.4	9.5	2.9	0.9	0.9
Saudi Arabia Basalt [6]	46.5	14.7	12.2	8.8	8.7	3.4	1.3	1.3
Colombia Andesite [40]	61.9	15.5	7.33	5.2	2.5	4.1	1.6	0.5
USA Dacite [50]	68.8	8.5	3.8	3.2	–	5.2	–	3.7
Japan Basaltic Andesite [51]	54.9	16.4	10.9	8.8	3.3	2.9	1.7	–

Saudi Arabia [52]	47	14.8	12.5	9.3	7.9	3.5	1.4	–
Algeria Andesite [25]	57.3	15	6	9	2	1.8	1.2	3.3
Turkey Tuff [22]	77.2	18.9	1.8	0.3	–	–	0.9	–
Jordan [27]	40.2	13.9	15.2	9.7	9.6	3.7	1.5	4.8
Greece Tuff [53]	69.7	12.2	2.3	2.0	0.7	0.6	3.3	7.4
General Range	40–70	10–20	1–15	2–10	1–10	1–5	1–5	<15

XRD Studies

X-ray Diffraction (XRD) analysis helps identify the mineralogical composition of volcanic ash. Minerals found in volcanic ashes originate primarily from magma and their composition depends on the magma chemistry and eruption conditions. The mineralogical composition can vary from almost amorphous to completely crystalline [43, 54].

- **Kupwade-Patil et al. (2016)** conducted XRD analysis on a raw volcanic ash and found the crystalline portion was made up of**:** anorthite sodian (16.9%), forsterite (9.9%), and calcite (1.5%). The amorphous component was determined to be 71.7% [54].
- The detection of calcium-rich zeolites such as thenardite further suggests elevated sulphate levels, which not only pose a risk of sulphate expansion but also provide nucleation sites that promote the formation of Calcium-Alumina-Silicate-Hydrate (C-A-S-H) gel in hybrid binders [54].

2.4.2 Global Availability and Accessibility of Volcanic Ash

Volcanic ash is widely available in regions with current or past volcanic activity, covering roughly 0.84 % of the Earth's land surface (about 124 million hectares), with 60 % of deposits in tropical climates. These deposits occur mainly as Andisols soils formed from volcanic ejecta in countries such as Indonesia, Italy, the USA, and New Zealand. While the global extent of volcanic ash is substantial, its accessibility for use in cementitious materials depends on factors like deposit depth, terrain, and required processing (cleaning, drying, milling). Below summarizes key regional sources and their logistical considerations [40].

- Pacific "Ring of Fire" countries - Indonesia, Japan, the Philippines, New Zealand, Ecuador (Otavalo), and the western USA - where frequent eruptions replenish fresh ash [55].

- Europe - Italy (e.g., Mount Etna) and La Palma in the Canary Islands with both historic and recent deposits [56].
- Africa - Ethiopia's Main Rift Valley (pumice/scoria), Kenya's natural pozzolans, Cameroon's "Cameroon Line," and the DRC's Nyamuragira shield volcano [47].
- Middle East - Saudi Arabia's Akhal Province holds basaltic ash suitable for activation [49].
- Central America - Guatemala and Colombia host extensive Andisol soils from past eruptions [19].

Economic and Logistical Challenges in Sourcing Volcanic Ash

The natural variation in mineralogical and chemical composition both across and within deposits necessitates detailed examination and characterization to confirm appropriateness for construction use [43]. Moreover, unrefined volcanic ash often necessitates considerable processing like cleaning, drying, milling, and sieving to reach the desired particle size and eliminate contaminants, a procedure that leads to high energy expenditure and might affect overall economic feasibility [32].

Further difficulties encompass elevated transportation costs resulting from the distant sites of numerous deposits and the significant upfront capital needed to establish the essential extraction, storage, and handling facilities. Concerns about contamination also emerge, especially in urban settings (e.g., ash gathered around Mount Etna may be tainted with oils and various materials), requiring additional cleaning and strict quality control procedures [57]. Additionally, the absence of uniform performance standards for volcanic ash, even with ASTM C618 in place, along with direct competition from more recognized supplementary cementitious materials such as fly ash and blast furnace slag, makes its sourcing even more challenging [35, 44],[14].

Despite these challenges, volcanic ash (VA) presents notable advantages in quarrying, ecological impact, and transport costs compared to other supplementary cementitious materials (SCMs). Quarrying VA typically involves surface-level extraction from naturally deposited pyroclastic materials, reducing the environmental disturbances and energy demands compared to conventional clay excavation methods. Additionally, VA use effectively addresses volcanic waste disposal issues, transforming post-eruption materials into valuable construction resources, thereby minimizing ecological impacts associated with landfilling. Unlike industrial SCMs such as fly ash or slag, volcanic ash deposits are often locally or regionally abundant, reducing energy consumption and greenhouse gas emissions associated with transportation over long distances. Moreover, VA typically requires minimal

processing energy relative to harder industrial by-products, thus further enhancing its environmental and economic viability as an SCM [7, 14].

2.5 Use of Volcanic Ash as Cement Replacement

2.5.1 Impact on Physical Properties of Mortar and Concrete

VA utilized as a supplementary cementitious material (SCM) can considerably affect the physical characteristics of mortar and concrete, such as water demand, workability, and setting time [58].

Workability

Multiple studies suggest that adding volcanic ash can influence the workability of concrete. The highest improvement in workability was noted with a 20% substitution of cement using VA [4]. Likewise, additional research on mortar indicated a small rise in slump flow (6%) with just the addition of VA, attaining peak flowability at 20% VA [15]**.** Nonetheless, other studies indicated that integrating VA at 15% and 30% cement replacement rates led to a reduction in flowability, no matter the fineness of the VA used [15]. A different study indicated that using up to 15% VA as a substitute for cement in concrete had a slight impact on the flow, but surpassing this replacement level decreased the flow [59]. These different outcomes indicate that the effect of VA on workability may be affected by elements like the replacement percentage, the particle size and origin of the volcanic ash, and the design of the mix [43].

Water Demand and Consistency

The water demand of a mixture is frequently connected to the desired consistency of the mortar. A study on mortar revealed that the standard of consistency diminished as the portion of cement replaced by VA increased [19]**.** This suggests a possible decrease in water demand at elevated replacement levels may occur to achieve a certain consistency.

Setting Time

Studies on mortar indicate that setting times rise with the increase in VA content in the mix, thereby highlighting the potential benefits of reduced heat of hydration during construction [19]**.** In particular, raising the VA content from 30% to 50% by cement weight prolonged the initial setting time from 140 to 190 minutes and the final setting time from 220 to 260 minutes [60]. A different study showed that the effect of VA replacement on both initial and final setting times was minimal up until a substitution rate of 40%, beyond which the setting times were extended [15]**.**

Bulk Density and Void Ratio

Research indicated that VA possesses a compacted bulk density of 1703 kg/m³ and an uncompacted density of 1499 kg/m³, exhibiting a void content of 13.61% [4]**.** Substituting more than 15% of cement with volcanic ash can lead to a decrease in the density of concrete samples cured in sulfate conditions, resulting in lighter concrete compared to standard mixes [4, 31].

The experimental results described above demonstrate that workability subtly changes with the proportion of replacement OPC or PC with VA and the properties of the VA, water demand diminishes, and setting times can extend.

2.5.2 Mechanical Performance of Volcanic Ash-Based Cement

Studies indicate that substituting a portion of OPC with VA significantly improves the development of concrete's compressive strength as time progresses. [18, 61-63].

The impact of VA on compressive strength is complex, depending on elements such as replacement ratio, particle size, water-to-binder ratio, and curing time [34, 48].

Numerous studies have indicated that adding VA to cement can improve compressive strength to an optimal replacement level typically between 10-20% after which strength usually decreases. As an illustration, research on mortar showed that substituting cement with volcanic ash enhanced the 28-day compressive strength by 27.7%, 7.8%, and 4.3% for replacement percentages ranging from 5% to 15%, respectively, before decreasing by 27.4% at a 20% substitution level [19, 31, 34]. This early enhancement is mainly due to the pozzolanic reaction, in which VA interacts with calcium hydroxide generated from cement hydration, resulting in the formation of extra cementitious substances like C-S-H and Calcium-Alumino-Silicate-Hydrate (C-A-S-H) gels [5, 15, 34, 54, 64].
On the other hand, certain studies indicate that the compressive strength often declines as the proportion of VA rises; nonetheless, they indicate that an ideal substitution up to 20% can yield desirable strength, typical consistency, and setting durations [34]**.** In a particular one [31], concrete blended with Sinabung's VA demonstrated that slight replacements of 2-4% could produce compressive strengths similar to, or even surpassing, those of standard concrete after 28 days.

The texture of the VA significantly influences its reactivity. Mortar mixes incorporating volcanic ash (approximately 6 µm particle size) as a partial replacement (up to 40%) for OPC have demonstrated a significant increase in compressive strength. These improvements attributable to the formation of a denser pore structure and the development of secondary C-S-H gels [21, 48, 65]. Additionally, the

development of long-term strength is frequently enhanced in mixtures that include VA due to the continuous pozzolanic reaction throughout prolonged curing durations, with lightweight aggregate concrete containing as much as 20% VA showing better compressive strength at later ages than control mixes [15].

Overall, the optimal replacement percentage of cement with volcanic ash to achieve satisfactory or improved compressive strength varies depending on the specific characteristics of the ash and the desired concrete properties. Many studies suggest that replacement levels up to 10-20% can be beneficial or comparable to control mixes, with some studies showing potential benefits up to 15-40% with optimized ash properties like particle size [5, 48, 58].

In general, although the ideal replacement percentage of cement with volcanic ash differs based on the unique attributes of the ash and the intended properties of the concrete, many studies indicate that replacement amounts between 10% and 20% yield the most advantageous enhancements in mechanical performance.

2.5.3 Durability and Long-Term Performance

The addition of VA to cementitious materials has demonstrated notable improvements in durability and long-term performance, especially in harsh environmental situations. A significant advantage highlighted in the literature is the enhancement in resistance to chloride penetration. Numerous studies indicate that the application of VA decreases the entry of chloride ions into concrete by improving its pore structure through the pozzolanic reaction [18, 28, 35, 63].

For instance, high-performance volcanic ash concrete (HPVAC) has shown significantly lower rapid chloride permeability than traditional mixtures and blended mixes, with finely ground natural basaltic ashes able to substitute as much as 50% of OPC demonstrating enhanced resistance to chloride penetration [19, 38, 57, 66]**.** Moreover, the decrease in the long-term chloride ion diffusion coefficient due to the inclusion of VA leads to improved corrosion resistance of the embedded steel reinforcement [19, 34].

Sulfate resistance is yet another field in which substitution of OPC with VA has demonstrated potential. Research on cement concrete blended with volcanic ash and pumice in sulfate-rich environments has revealed that substituting some cement with VA provides some resistance to sulfate damage [5, 43, 67]. Significantly, concrete mixes with over 15% VA and cured in harsh H_2SO_4 and $MgSO_4$ conditions showed decreased density an effect associated with the blend's durability performance [4].

Additionally, studies on the corrosion resistance of steel reinforcement in VA-blended cement mortars show that incorporating VA, even at substitution rates of 20% to 40%, can improve durability by reducing long-term chloride ion penetration [57, 68, 69]. This enhanced performance is essential for extending the durability of reinforced concrete structures, especially in environments rich in chloride. Although there is a scarcity of explicit carbonation tests on volcanic ash concrete in the current literature, it is widely anticipated that the improvement of the pore structure resulting from the pozzolanic properties of VA will decrease CO_2 permeability, thus improving resistance to carbonation [70].

The development of the microstructure in replacement of VA for OPC is crucial for these enhancements in durability. Examinations utilizing XRD, SEM, and Mercury Intrusion Porosimetry (MIP) have repeatedly shown that the persistent pozzolanic reactions result in the development of secondary C-S-H and C-A-S-H gels [15, 36, 48, 54, 64, 65]**.** These gels occupy the capillary gaps inside the cement matrix, leading to a more compact, less permeable structure that more effectively withstands the intrusion of aggressive ions and other detrimental materials.

In conclusion, utilizing volcanic ash as a substitute for cement not only boosts the concrete's resistance to chloride infiltration and sulfate damage but also aids in enhancing corrosion resistance and long-term durability. These advantages are mainly linked to the better microstructural densification from the pozzolanic reaction of VA, resulting in improved performance under harsh conditions.

2.6 Use of Volcanic Ash as Alkali-Activated Cement (AAC)

Volcanic ash (VA) is becoming a potential precursor for alkali-activated materials (AAM), providing an eco-friendly substitute to conventional Portland cement (OPC) with notable environmental and financial advantages [14, 41, 43, 71]. The vast number of untapped VA deposits globally makes it a significant aluminosilicate geo-resource for manufacturing AAC, exhibiting beneficial densification characteristics, mechanical properties, and minimal porosity.

2.6.1 Classification of Alkali Activated Volcanic Ash Binders:

The alkaline activation of VA can generally be divided into two main categories as detailed below

1. Geopolymers (Inorganic Alkaline Polymers)

In these systems, VA is triggered without OPC, leading to the creation of a three-dimensional aluminosilicate framework. The primary reaction products typically consist of sodium aluminosilicate

hydrate (N-A-S-H) or potassium aluminosilicate hydrate (K-A-S-H) gels, occasionally alongside zeolitic deposits [14].

2. Hybrid Cements

These systems include a small amount of OPC combined with a large amount (usually exceeding 70%) of VA as an aluminosilicate precursor. The products of the reaction are intricate cement-like gels that merge the hydration of OPC with the alkali activation of VA [14].

2.6.2 Suitability of Volcanic Ash for AAC

For VA to serve as an effective precursor for AAC, specific compositional parameters are essential. VA is deemed appropriate when its total SiO_2 and Al_2O_3 concentration is a minimum of 70%, with a SiO_2/Al_2O_3 molar ratio ranging from 3.3 to 4.5 and an amorphous phase proportion surpassing 36% [47, 71]. Additionally, the reactivity of VA is boosted by elements like a high content of reactive SiO_2, a larger specific surface area, structural irregularities, and an elevated amorphous fraction [43].

2.6.3 Methods to Improve Volcanic Ash Reactivity

To address the inherently low reactivity of certain volcanic ashes, various activation methods are utilized.

- Mechanical activation - Extended grinding increases surface area and breaks down crystalline structures, which enhances reactivity and strengthens development in AACs [7, 14, 47, 72, 73]. Prolonged grinding can improve the specific surface area, potentially mitigating longer setting times and lower early strengths associated with volcanic ash use [43].
- Thermal activation - Calcination within the 700 -1000 °C range, has shown effectiveness; for instance, pumice preheated to 1000 °C markedly enhanced pozzolanic activity and compressive strength in blended systems [7, 24, 74]. However, this method must be balanced against increased energy consumption and associated CO_2 emissions resulting from the high-temperature treatment [74].
- Chemical activation - Compounds like calcium chloride ($CaCl_2$) or sodium silicate (Na_2SiO_3) have been demonstrated to enhance early-age strength in VA-based mortars [7]. Additionally, curing at higher temperatures (e.g., 40 - 90 °C) speeds up geopolymerization and encourages the development of strength-enhancing gel phases, even in volcanic ashes with minimal amorphous content [47].

Moreover, mixing VA with additional reactive substances like metakaolin, slag, or fly ash can further improve the effectiveness of the final binder system [14, 75-77].

2.6.4 Activation Methods in VA- Based AACs

The alkali activation of VA encompasses a sequence of dissolution, reorganization, and polymerization processes. In sodium-based systems, amorphous silica and alumina from VA dissolve at high alkalinity (usually with NaOH or Na_2SiO_3), yielding silicate and aluminate species that polymerize into a N-A-S-H gel - a three-dimensional structure stabilized by sodium ions [67, 78].

When calcium is added via the VA itself, OPC, or calcium-containing activators the reaction pathways expand to encompass C-S-H and C-A-S-H gels [14, 36, 54, 71]. In these hybrid systems, calcium hydroxide produced from the hydration of OPC reacts with soluble silicates and aluminates to create dense, calcium-rich gel phases. Mixed N-(C)-A-S-H phases form in strongly alkaline conditions (e.g., 10 M NaOH), whereas C-S-H gels prevail in moderately alkaline environments (e.g., 2 M NaOH) [29, 79].

2.6.5 Impact of Alkaline Activators on Reactivity and Gel Formation

Table 3 summarizes the key advantages and disadvantages of commonly used chemical activators in VA for OPC to enhance its reactivity. The kind and amount of alkaline activator are essential in influencing the dissolution kinetics of VA and the properties of the final binder [47, 72, 80]. Sodium and potassium hydroxides (NaOH, KOH) are efficient in starting the dissolution of amorphous phases, whereas sodium or potassium silicates supply extra silica, which aids the polymerization process and strengthens mechanical properties [14, 47]. The final microstructure, setting time, and strength development are affected by the viscosity, modulus (SiO_2/Na_2O), and reactivity of these activators.

Table 2 Advantages and disadvantages of different chemical activators with volcanic ash

Activator Type	Advantages	Disadvantages	Sources
NaOH	Fast dissolution of aluminosilicates; high early strength in some cases	Efflorescence risks; safety concerns; may lower ultimate strength	[14, 47]
KOH	Similar to NaOH	Costlier; less studied in VA systems	[14]
Na_2SiO_3	Provides soluble silica; denser gels; improved strength	High viscosity; may reduce workability	[14, 47]
$CaCl_2$	Enhances early-age strength in VA mortars	Long-term durability needs further study	[7]
Na_2SO_4	Positive strength impact in hybrid binders	Requires combination with other activators	[7, 80]

The ideal mix of activators greatly relies on the chemical composition, mineral content, and particle traits of the volcanic ash, along with the specific use of the AAC [14, 47, 72].

2.6.6 Practical Applications of Volcanic Ash based AAC

Volcanic ash (VA)-based alkali-activated concretes (AACs) have demonstrated considerable potential for various sustainable construction applications. These include the production of low-carbon self-consolidating concrete (SCC) with up to 50% cement replacement, achieving strengths of at least 15 MPa and suitable durability for structural use [7, 36, 49, 54, 69]. VA-based AACs have also been investigated for repair mortars, marine structures, lightweight precast units, and geopolymer concrete and mortar applications. Although large-scale case studies are limited, extensive laboratory and pilot studies confirm the practicality of VA-based AACs in diverse structural and environmental contexts. Additionally, historical use of volcanic ash in Roman concretes underscores the long-term durability of these binders, supporting their viability in modern sustainable construction.

These binders**,** primarily volcanic ash (VA)-based alkali-activated concretes (AAC) and hybrid systems combining VA with OPC or other SCMs, have demonstrated application potential in various contexts:

- Repair mortars - Binary alkali-activated mortars incorporating natural volcanic pozzolan have been proposed for use in structural repair, showing adequate mechanical performanceMortars for repair made with natural volcanic pozzolan [57, 65, 81].

- Marine structures - VA-blended cement concretes exhibit improved durability in chloride-rich marine environments, extending service life [35, 44, 82].
- Lightweight masonry units - Lightweight concrete featuring volcanic slag aggregates either alone or blended with VA has been used in the production of high-performance masonry blocks [69, 83, 84].
- Geopolymer mortars - VA serves as a precursor in geopolymer systems, where strength and durability characteristics can be tailored by adjusting activator types and curing regimes [47, 48, 85].
- Geopolymer mortars - VA serves as a precursor in geopolymer systems, where strength and durability characteristics can be tailored by adjusting activator types and curing regimes [7, 8, 61].

Although extensive field-scale applications are still being developed, the literature indicates significant potential for these materials in both traditional and specialized construction markets. Significantly, the Romans' historical use of pumiceous volcanic ash with hydraulic lime known as hydraulic pozzolanic cement, led to the long-lasting structures in the Bay of Naples, which still endures today [49, 54]. In modern contexts, VA-blended concretes including alkali-activated and hybrid formulations have been proposed as economical and sustainable solutions for infrastructure rehabilitation in volcanic disaster-prone regions [69].

2.7 Use of Volcanic Ash as Hybrid Cement Binders

2.7.1 Hybrid Systems Combining Volcanic Ash and Ordinary Portland Cement

The use of volcanic ash (VA) as a partial substitute for ordinary Portland cement (OPC) in hybrid cement systems has attracted notable attention because of its technical viability and ecological benefits. Hybrid systems seek to utilize the combined advantages of the pozzolanic properties of VA and the hydraulic reactivity of OPC, resulting in superior mechanical performance and increased durability [5, 64, 86].

Numerous studies have explored different degrees of OPC replacement with VA. Hossain [87] assessed mixtures containing as much as 50% VA and noted significant pozzolanic reactivity attributed to a high silica level (~60%). Substituting VA by as much as 50% resulted in microstructural densification through the development of C-S-H and C-A-S-H gels [54]. Optimal replacement levels between 10% and 30% provided the best mechanical and microstructural results [58]. Moreover, the use of portlandite in pozzolanic reactions enhances durability by decreasing vulnerability to sulphate attack and leaching

[5, 64]. The corrosion resistance and chloride diffusivity of VA blended cement mortar have also been specifically investigated [68].

The reactivity of VA is also affected by its particle size. Smaller VA particles show increased surface areas, boosting pozzolanic activity and aiding in improved strength formation. Studies have indicated that decreasing the particle of VA notably enhances its reactivity and the effectiveness of blended cements [82, 87] [46, 48].

2.7.2 Effects of Activator Type and Quantity on Binder Performance

Although OPC hydration products can trigger the pozzolanic reaction of VA, employing chemical activators can improve binder performance by fostering early reactivity and strength development. These activators consist of alkaline substances and sulphates, which aid in the dissolution of reactive VA phases and speed up the creation of binding gels.

Lopez-Salas and Escalante-Garcia (2024) [8] studied hybrid cements that incorporate volcanic pumice, ordinary Portland cement (OPC), and chemical activators like sodium sulphate (Na_2SO_4) and calcium hydroxide. Their results showed that the VA content affected initial strength, whereas the activator formulation greatly influenced strength growth over time. Significantly, the molar ratio of Na_2SO_4 to $Ca(OH)_2$ played a vital role in optimizing strength, and increased amounts of Na_2SO_4 did not consistently produce superior outcomes.

Further studies have investigated alkali activation in high-VA-content systems nearing geopolymer-type reactions [73, 79, 85, 88]. Although usually examined in environments without OPC, the principles of alkali activation can enhance hybrid binders containing lower OPC levels by increasing pH and facilitating the dissolution of aluminosilicate phases [71].

The quantity of chemical activators should be precisely regulated. High levels of activator can cause negative outcomes including quick setting, shrinkage, or cracking [8]. For example, research conducted by Hossain and Lachemi (2007) [64] showed that although VA improves durability, it could also lead to increased drying shrinkage because of a finer pore structure and higher water requirements. This can be alleviated by careful mix design and improved curing conditions [69].

2.7.3 Microstructural and Sustainability Analysis

Characterizing microstructures is essential for comprehending the performance of VA-OPC hybrid systems. SEM, XRD, FTIR, and Nuclear Magnetic Resonance (NMR) offer understanding of hydration processes, gel creation, and microstructural evolution [8, 36, 54].

SEM investigations indicate that the addition of VA results in the creation of dense C-S-H and C-A-S-H gels, which occupy voids and enhance the pore structure [33, 45]. The incorporation of VA enhances microstructural densification as curing time progresses [54]. Likewise, improved microstructural uniformity and density at optimal VA levels [58].

XRD analyses demonstrate a decrease in portlandite peaks with the addition of VA, signifying efficient pozzolanic utilization of $Ca(OH)_2$ [36, 46, 54]. FTIR findings confirm the existence of silicate and aluminate connections linked to the development of binding gels [8, 54], whereas NMR provides additional insights into the local atomic environments of hydration products, such as the coordination of C-A-S-H gels and the degree of polymerization of the silicate chains [8, 36, 54].

Replacing OPC, a material that requires a lot of energy and emits carbon, with volcanic ash decreases both embodied energy and CO_2 emissions [21, 79]. Performed life cycle assessments discovered that replacing up to 40% of OPC with finely ground VA could lead to a 16% decrease in EEC [21, 36].

In addition, utilizing locally sourced volcanic ash decreases transportation energy and encourages the valorisation of natural or industrial by-products, improving circularity and resource efficiency [49, 54, 69]. In areas vulnerable to disasters caused by volcanoes, self-consolidating concrete (SCC) made from volcanic ash (VA) has been suggested as an affordable and eco-friendly option for developing and restoring infrastructure [69].

CHAPTER 3. MATERIALS, METHODS & EXPERIMENT DESIGN

This section presents the experimental investigations carried out to evaluate the influence of activator powders on the performance of hybrid cementitious binders incorporating volcanic ash (VA) and Portland cement. Two experimental series were designed: In series A, both activator powders were varied in amount, and then based on those results NS/CH was kept constant at 1 and NS percentage was varied in series B. These experiments aim to assess how chemical activation (using Na_2SO_4 and $Ca(OH)_2$) and mechanical processing (e.g., grinding of VA) affect hydration behaviour, strength development, and microstructural evolution. This work aligns with the broader research objective of developing more sustainable binder systems with reduced clinker content.

3.1 Description of Materials

3.1.1 Cement

The cement utilized in this study was Ultracem, which is a general-purpose Portland Cement (Type GP) that complies with the standard NZS 3122:2009. It is appropriate for a range of construction requirements and was chosen for its reliability and suitability for the application of supplementary cementitious materials.

XRF was used to analyze the chemical composition of the GP cement, as shown in Table 4. Notably the cement contains high CaO content (64.5%), which is important for clinker reactivity and plays a role in strength development in the hybrid binder.

Table 3 Chemical composition of GP cement

Compounds %	SiO_2	Al_2O_3	TiO_2	Fe_2O_3	MgO	Cao	Na_2O	K_2O	SO_3
Composition	20.3	5.59	0.3	3.13	0.97	64.5	0.29	0.35	2.06

A scanning electron microscopy (SEM) micrograph is presented in Fig. 22, and shows the microstructural characteristics of the cement particles, with their irregular morphology and surface texture, both of which are important to their reactivity and hydration kinetics. Fig. 11 is a photograph of the Holcim Ultracem cement used in the experimental work, which shows the raw commercial product tested for reproducibility and transparency reasons.

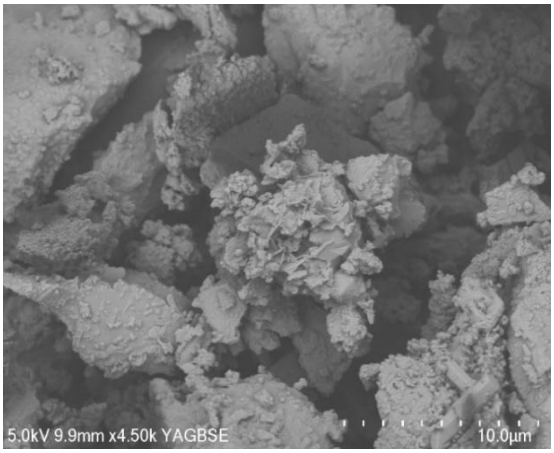

Fig. 2. SEM image of the cement

Fig. 1. cement used in the experimental work

An analysis of particles was performed to assess the particle size distributions and specific surface area of volcanic ash and cement, to assess their suitability for use in replacement experiments. The particle size distribution was determined using a Malvern Mastersizer Xplorer (v5.02) at the university laboratory, following standard dispersion protocols. The analysis showed that 100% of the cement particles measured 150 µm, with the specific surface area is 365 m^2/kg.

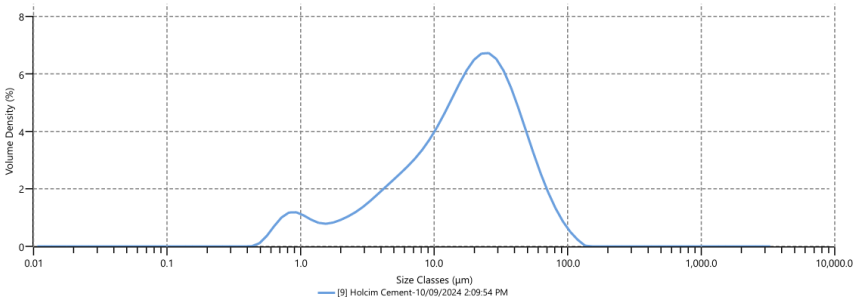

Fig. 3. Particle size distribution of the GP cement

3.1.2 Volcanic Ash

The rhyolitic volcanic ash (Hamilton Ash) used in this research was sourced from the Takitimu North Link (TNL) project in Tauranga, New Zealand (Fig. 4), for ease of reference it will hereafter be referred to as volcanic ash (RVA).

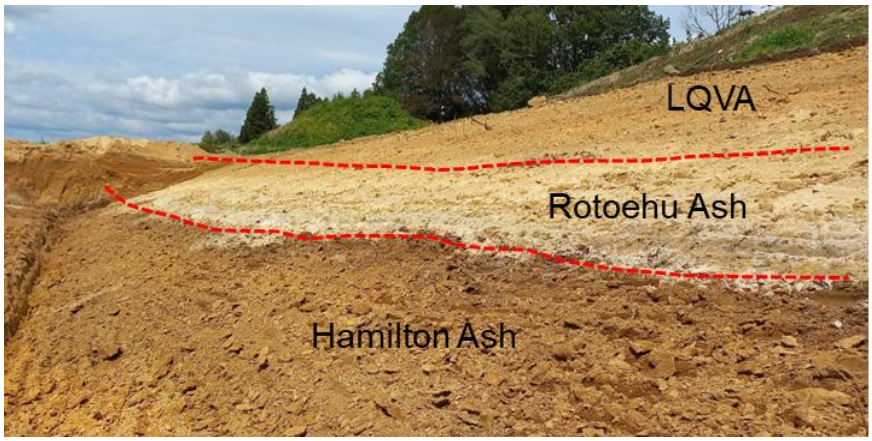

Fig. 4. Volcanic Ash beds at the TNL sampling site, where LQVA (Late Quaternary Volcanic Ashes (Photograph credit Berrick Fitzsimons (Beca Ltd.)).

The Hamilton Ash formation comprises a sequence of highly weathered, clay-textured tephra beds and paleosols, prominently found in the Waikato, South Auckland, and Tauranga regions Fig. 4.

This sequence of ashes is divided into eight units, labeled H1 (bottom) to H8 (top), though typically fewer than eight units are present at any given site. At Omokoroa in the Bay of Plenty, the Hamilton Ash reaches a thickness of approximately 2.5 metres, but it is generally around 1 metre in thickness, likely due to erosion of the beds and paleosols. The H1 unit has been identified as the Rangitawa Tephra (in the southern North Island), with a zircon fission track age of 0.35 ± 0.04 million years [89].

Fig. 5. distribution of the Hamilton Ash Deposits in the North Island of NZ (sourced from Google map)

Table 4 Chemical composition of the VA

Compounds %	SiO_2	Al_2O_3	TiO_2	Fe_2O_3	MgO	Cao	Na_2O	K_2O	SO_3
Composition	43.37	30.24	0.73	6.77	0.21	0.641	0.98	0.07	0.03

The particle size distribution of the volcanic ash (VA) sample was evaluated before and after mechanical grinding. Initially, only 30% of the particles measured under 150 µm in diameter, and the specific surface area was 48.97 m²/kg. After grinding the VA sample for three minutes, the results showed a significant improvement, with approximately 83% of the particles falling below 150 µm and an average specific surface area increasing to a range of 350-400 m²/kg. This enhancement demonstrates the effectiveness of the grinding process in refining particle size and increasing surface area, both of which are critical for improving pozzolanic reactivity.

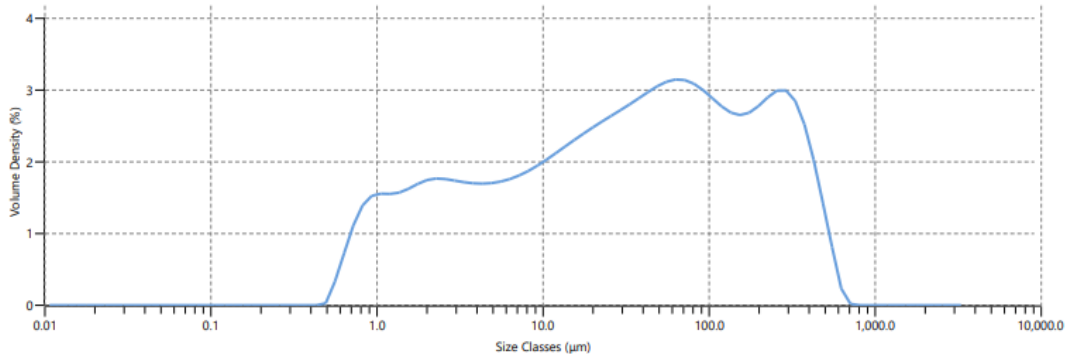

Fig. 6. Particle size distribution of the VA particle

These improvements in fineness and surface area significantly enhance the physical characteristics of volcanic ash with ordinary Portland cement (OPC). It has been shown [52] that finer volcanic ash particles contribute to a denser pore structure in cured cement pastes. The findings suggest that volcanic ash, when finely ground, can align with the physical properties of cement.

To evaluate the suitability of the VA for use in cementitious material, key physical and geotechnical properties were measured. The specific gravity of the volcanic ash used in this research is 2.296, Its liquid limit is 123.21%, the plastic limit is 88.15% and the resulting plasticity index is 35.09% signifies a material with comparatively low plasticity. Moreover the, the linear shrinkage was recorded 20%.

The following SEM images of the volcanic ash (Fig. 7 (a) & (b)) further illustrate the angular morphology and irregular surface texture of the particles

Fig. 7. raw volcanic ash sample

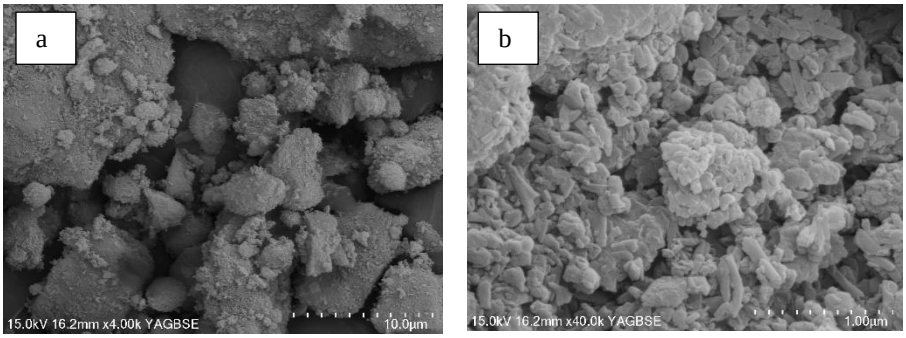

Fig. 8. (a) & (b) SEM images of Volcanic Ash

3.1.3 Activators

In this series of experiments Calcium Hydroxide (CH) and Sodium Sulphate (NS) have been used as activator powders. The selection of NS and CH as activators was based on their synergistic chemical mechanisms. CH increases pH and provides calcium ions, promoting the formation of C-A-S-H-type phases, while NS enhances early-age strength via ettringite formation in systems rich in reactive aluminates [8].

Compared to highly alkaline alternatives such as NaOH or Na_2CO_3, the NS/CH system was selected for its lower handling risk and environmental impact, as well as its compatibility with the hybrid binder system under ambient curing conditions.

3.1.4 Water

The water used in the mixtures was sourced from the University of Waikato's concrete laboratory. It originated as tap water supplied via the potable water network installed and maintained by Hamilton City Council in New Zealand. The same water was also used for curing the concrete samples after casting.

3.1.5 Aggregates

Cemex sand in New Zealand is a high-quality aggregate used extensively in construction for its consistency and reliability. It is sourced from natural deposits and processed to meet specific project requirements, ensuring optimal performance in concrete, asphalt, and other building materials.

3.1.6 Preparation of Materials

Both fine aggregates (sand) and volcanic ash were required to be dry. This is crucial because the moisture content of the aggregate affects the actual free water content in the mix. To ensure proper moisture content, these materials were dried in an oven at 100°C for 24 hours. The dried volcanic ash was then ground with a ball mill grinder in the university laboratory for 3 minutes to produce particles of less than 150µm, which are required for the experiment.

Fig. 10. Ball mill grinder

Fig. 10. Ground VA

3.1.7 Preparation of Sample

The mortar mixtures were prepared using a 5-litre capacity Kensington stand mixer. A systematic mixing procedure lasting 8 minutes was undertaken to ensure a standardized mix. All dry ingredients (cement, volcanic ash, sand and activator powders) were initially mixed for 1 minute, followed by the addition of half of the required water quantity, Mixing continued for 1 additional minute to initiate hydration.

Fig. 11. Kitchen hand mixer used for sample preparation

The gradual addition of the remaining water was undertaken while mixing for 2 minutes, followed by scraping the bowl with a metal spatula and then mixing to create some uniformity using a metal spatula for 1 minute. A final period of mixing for 3 minutes completed the homogenization process. The mixed specimens were then immediately turned into 50×50×50 mm cube moulds in three layers. Each layer was compacted using tamper before adding the following layer. After completing the final layer any excess material was removed from the top surface of the mould with a trowel and surface smoothed. The moulds were then covered with a plastic film to avoid water loss.

3.1.8 Preparation of Moulds

Before mixing the concrete, the moulds were required preparation prior to casting the samples. Fig. 122; illustrates the moulds used in this study for compressive strength testing. Each mould was thoroughly cleaned and screws were tightened to ensure precise dimensions during casting. The inner surfaces were coated with a Sika Formol, a concrete releasing agent to facilitate the demoulding process after the concrete had hardened.

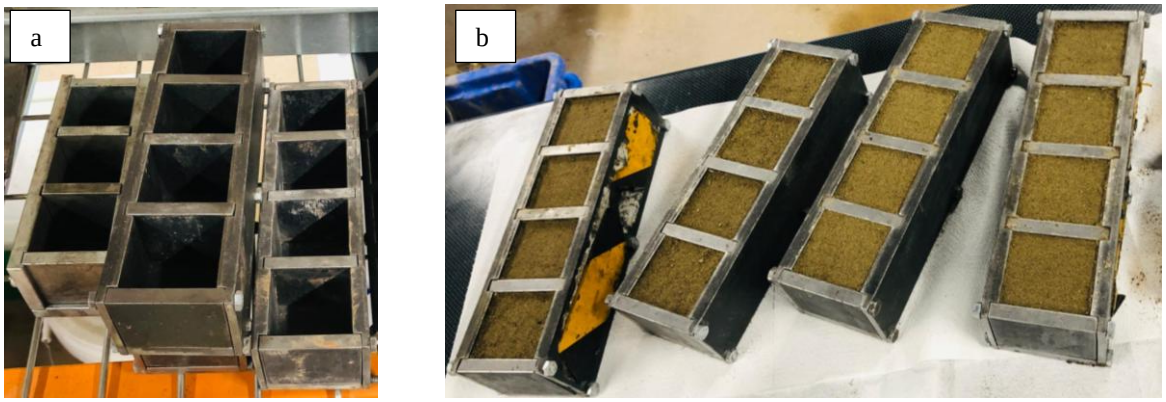

Fig. 12. (a) Moulds used for casting (b) Moulds filled with the VA-hybrid

3.1.9 Demoulding and Curing Details

The cast specimens were demoulded approximately 18 to 24 hours after mixing. After removal from the moulds, the samples were labelled according to their mix design and intended curing duration, as shown in the Fig. 14. The labelled specimens were then placed in a curing tank filled with portable water, as shown in Fig. 14. The curing tanks were maintained at a constant temperature of 23°C. The specimens were cured in these conditions until they reached the predetermined lengths of curing time required prior to compression testing at 7, 28, and 90 days.

Fig. 14 Water tank used for curing samples at a constant temp.

Fig. 13 Samples for curing for 7,28 and 90 days

3.2 Methods of Testing

3.2.1 Specific Gravity Test (Solid Density)

Specific gravity is the ratio of the weight of a given volume of aggregate (soil) to the weight of an equal volume of water. The test was conducted according to NZS 4402:1986 Test 2.7.2. Equation (1) was used to determine the specific gravity.

The apparatus used for this test included a balance, density bottles, a water bath, and a vacuum pump. For the procedure, approximately 200 g of soil was used, with each density bottle filled with 20 g of soil in two equal portions. Air-free distilled water was then added to the bottles until the water level covered the soil to a depth of 10–20 mm. Care was taken to ensure that all soil was washed down to the bottom of the bottle. The bottle was then connected to a vacuum pump, and the pressure was gradually reduced to remove trapped air. Once the release of air became less vigorous, the bottles were gently warmed in a 25 °C water bath to complete the deaeration process.

$$\boldsymbol{G = \frac{M_2 - M_1}{(M_2 - M_1) - (M_3 - M_4)}} \qquad (1)$$

Where,

M_1 = mass of empty density bottle

M_2 = mass of empty density bottle and dry soil

M_3 = mass of density bottle, soil and water

M_4 = mass of density bottle filled with water only

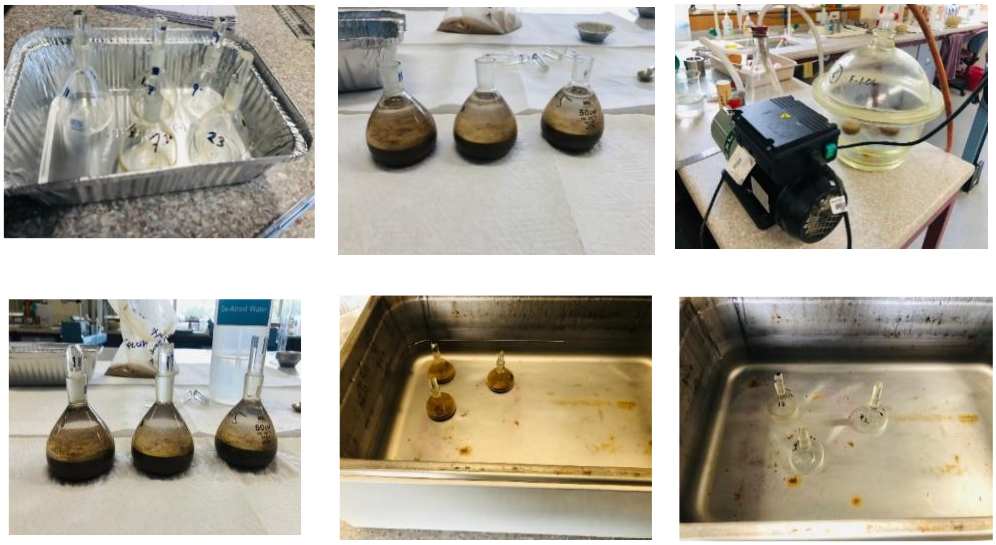

Fig. 15. Specific gravity test setup

3.2.2 Cone Penetration Limit (Liquid Limit)

The liquid limit of the volcanic ash was found using the cone penetration limit test according to New Zealand Standard NZS 4402.2.5:1986 by measuring the depth of penetration of a standard cone into the sample.

The test was preceded by air-drying the soil and then sieving it through a 425µm sieve before mixing it with distilled water to form a paste. Different water contents were used to prepare pastes with varying workabilities. Each paste was placed into a cone penetration test cup having a smooth, clean surface. The conical point positioned (Fig. 18) so its tip just touched the surface of the paste and then released to penetrate under its own weight for 5 seconds (Fig. 17). Penetration was measured to the nearest

Fig. 17 before releasing the conical point

Fig. 16 After penetration

0.1mm. This procedure was repeated for five different moisture content levels. In addition, a portion of each paste was oven-dried at 105 ± 5 °C to determine its moisture content (Fig. 19.)

The liquid limit was taken as the value of the moisture content equivalent to 20mm penetration depth by the cone, as per NZS 4402.2.5:1986. To obtain this value a best-fit curve was constructed through the test points, and the liquid limit was designated at the point of intersection between the curve and the 20 mm penetration line.

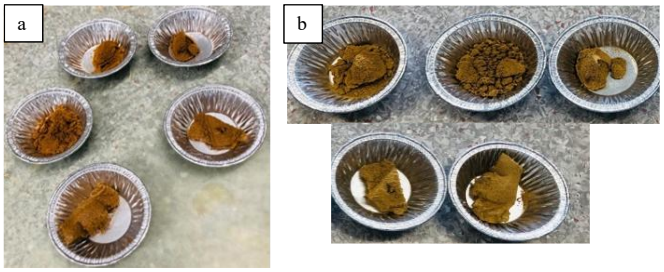

Fig. 18 (a) samples before oven dry and (b) after oven

3.2.3 Plastic Limit

The plastic limit test was conducted in accordance with NZS 4402.2.3:1986 to determine the minimum moisture content at which the volcanic ash transitions into a plastic state.

The procedure involved air-drying the sample and sieving it through a 425-micron sieve before mixing with distilled water until a workable consistency was achieved. Small portions of the paste were rolled by hand between glass plates into threads. When the threads fractured at a diameter of approximately 3.2 mm, the corresponding moisture content was recorded. If breakage occurred at a larger diameter, the sample was remixed with additional water and retested. Several trials were performed, and the average of the recorded values was reported as the plastic limit.

A portion of each prepared paste was oven-dried (Fig. 20) as per standard requirements to determine its total moisture loss, which contributes to understanding the consistency and drying behaviour of the material under test conditions.

$$PI = LL - PL \qquad (2)$$

The plasticity index (PI) was computed from the equation (2) in which LL is the liquid limit and PL is the plastic limit. The value of plasticity index calculates as percentage, which is [description based on PI, low, medium, or high plasticity]. This parameter is essential for soil classification and geotechnical evaluation, as it offers insights into the material's compressibility, strength, and volumetric behaviour under varying moisture conditions.

Fig. 19 Threads before oven dried

3.2.4 Linear Shrinkage

A test of linear shrinkage was conducted to determine the potential for shrinkage of the soil when dried. The test involved the preparation of a paste, which consisted of mixing air-dried and sifted soil (which passed through a 425-micron sieve) with distilled water. The mixture was done until it yielded a homogeneous and smooth paste. The paste was filled into a calibrated shrinkage mould and evenly spread so that it had no air bubbles. The mould was left under a controlled condition to dry.

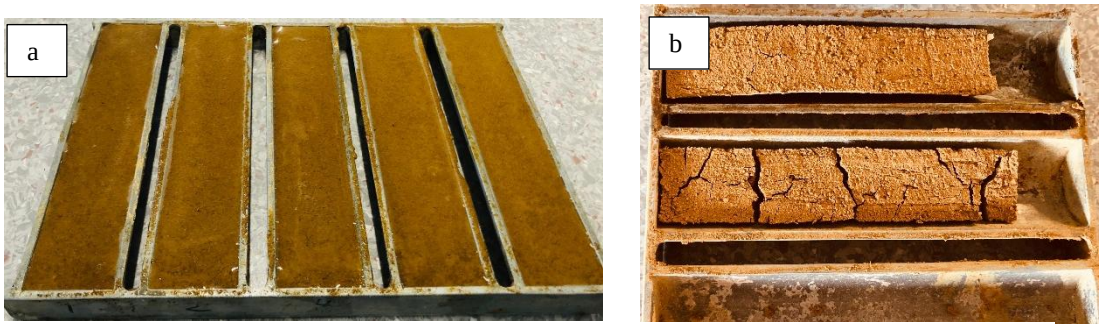

Fig. 20 (a) before and (b) after drying samples

After the process of drying is completed and a constant length has been achieved, length shrinkage was measured using a vernier caliper. The linear shrinkage percentage was calculated based on the following formula: The results show that the sample of volcanic ash has a linear shrinkage of 20%, and this shows [value-based conclusion, e.g., high shrinkage value or low shrinkage value].

The linear shrinkage test gave useful data on the volumetric stability of the soil when dried, which is important in determining its constructability. Combined with liquid and plastic limits, this data forms a full soil classification test.

3.2.5Flow Table Test

The flow table test was conducted following the guidelines outlined in ASTM C1437 to evaluate the workability as well as consistency of cement replacement mixtures. This standard was selected because there is no equivalent New Zealand Standard (NZS) specifically covering flow table tests for cementitious pastes, and ASTM C1437 is widely accepted for such assessments in both academic and industry practices.

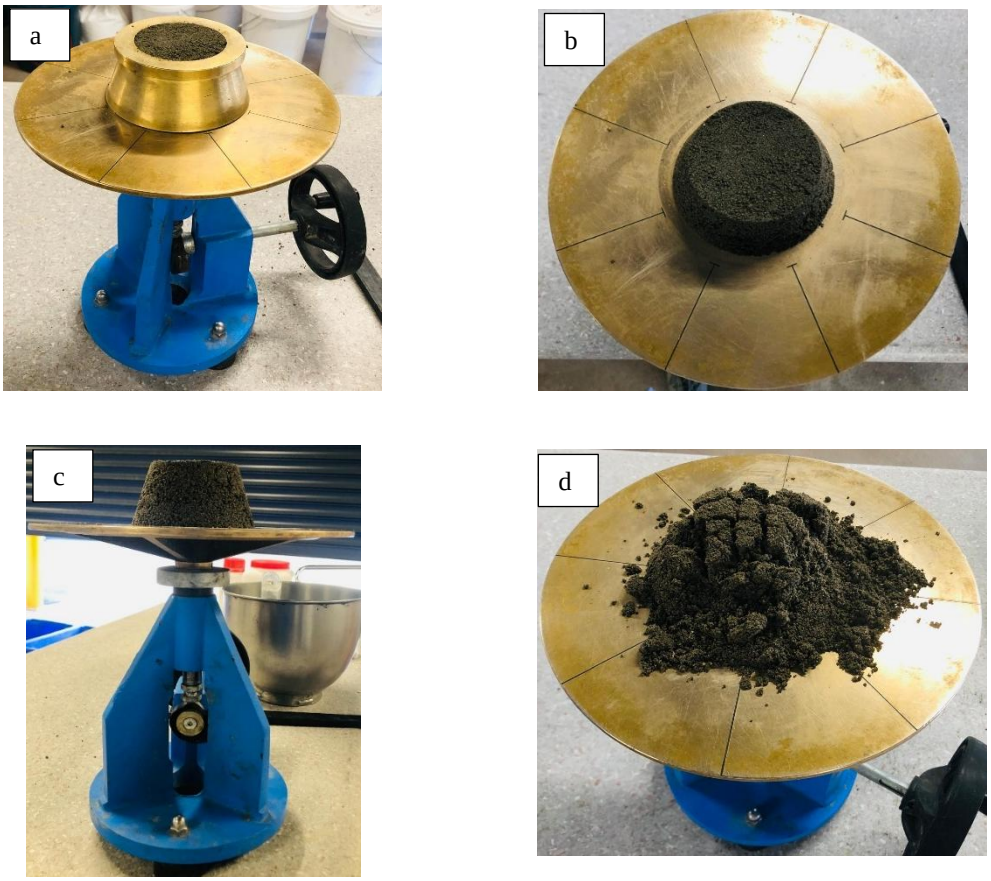

Fig. 21 Flow table setup and spread test process (a) Initial placement of cement paste in flow table mould; (b) Top view of filled mould before flow; (c) Side view showing moulded paste ready for flow table drops; (d) Final spread of paste after flow table drops

The flow table test was performed using a standard flow table apparatus. Every mixture was subjected to 25 consistent drops onto the flow table; after it, the average diameter of the spread (flow diameter, D) was measured in millimeters (mm). The mixtures were carefully prepared according to certain mixing procedure described in the sample preparation section to ensure homogeneity and reproducibility.

3.2.6 Initial and Final Setting Time

The initial and final setting times are critical indicators of the workability and early-stage hydration behavior of cementitious materials. These parameters influence how long a binder remains workable and when it begins to harden, which is important for casting, finishing, and structural performance.

The initial and final setting times were measured using the Vicat apparatus according to ASTM C191, as no direct equivalent exist in the current New Zealand Standards (NZS). The initial setting time was measured as the duration of the time from the addition of water to the binder to when the Vicat needle no longer penetrated to a depth of 25 mm. The final setting time was recorded when the Vicat needle ceased to visibility penetrate the surface of the sample.

3.2.7 Compression Test

Although durability and permeability are critical factors in real-world applications, compressive strength remains one of the most fundamental and widely assessed mechanical properties of concrete and mortar. Compressive strength tests, following ASTM C109, were performed at 7, 28, and 90-days following placement of the cast samples in the curing tank.

Each specimen was centred on the lower platen of the PILOT PRO ASTM Automatic Compression Tester for Blocks to ensure even load distribution during testing. The compressive force was then applied gradually until the specimen failed, either by collapsing or cracking, as shown in Fig. 23.

Fig. 22 Test set up for compressive strength of mortar

Fig. 23 shear failure for one of the samples.

3.2.8 SEM Sample Preparation

The study performed SEM analysis using Environmental Field Scanning Electron Microscopy (E-SEM). SEM analysis was performed on unpolished samples to study their microstructure while polished samples underwent examination using BSE. A resin base was created for polished samples using epoxy base 105 mixed with a West System hardener. The sample polishing process involved sanding the samples using sandpaper with grit size 500 followed by 1000, 2000 and finally 4000. The samples received a platinum coating before placement into the machine following the polishing process. The magnification level was adapted to attain the necessary resolution to enable precise documentation of surface morphology.

Fig. 24 Prepared samples for SEM analyses.

3.2.9 FTIR Sample Preparation

Fourier transform infrared (FTIR) spectroscopy analyses the initial composition and its modifications during the curing process, revealing physical and chemical transformations caused by curing environments. Sharp, clear bands in FTIR spectra result from crystalline substances, while glassy materials produce wide peaks, with amorphous materials lying in between these two extremes [90] .

For the FTIR analysis, fragments of the samples from the 28-day compression test were used to ensure a direct link between the structural changes seen spectroscopically and mechanical behavior.

3.2.10 XRF Sample Preparation

XRF analysis was carried out on both the volcanic ash and cement to determine their chemical composition. For the XRF, samples (RVA) were dried overnight at 100-105°C to drive off moisture. Thereafter, the bulk samples were ground to a fine powder. LOI (Loss On Ignition) was measured by heating 1–2g of the sample at 1100°C for 1 h and water content was calculated from the weight gained or lost, reported as a percentage. The fused beads for major oxide element analysis are prepared with a flux-to-sample ratio of 10:1 (8 g flux: 0.8 g sample ± 0.0030). The fusion was carried out in the Claisse Neo Fluxer furnace at 1050°C in the presence of a releasing agent, 0.1–0.2 g of NH4I (ammonium iodide). The flux is 57% lithium tetraborate and 43% lithium metaborate, "54:43". The samples were analyzed on the machine Bruker S8 Tiger (WDS), located in the School of Science at the University of Waikato.

Fig. 25 sample before insertion into furnace and after colling

3.2.11 XRD

X-ray diffraction (XRD) analysis was performed to detect the mineral composition of mortar mixes. Samples were obtained from the 28-day compression test. XRD analysis was performed using a PANalytical Empyrean Series 2 diffractometer with Cu Kα radiation (λ 1.5406 Å), a nickel foil filter at 40 kV and 30 mA. The XRD patterns were obtained by a scanning rate of 1° per minute from 2θ 5° to 90°.

Fig. 26 Claisse Neo Fluxer Furnace

3.2.12 TGA/DTA

TGA was performed on powdered samples obtained from 28-day hardened pastes. A Netzsch STA 449 F5 Jupiter instrument was used to perform TGA on the samples, covering a temperature range of 30°C to 800°C with a heating rate of 10°C/min. This procedure enabled the identification of weight loss events and decomposition temperatures, providing insights into hydration products, carbonate content, and thermal stability. The TGA/DTA results were used to evaluate the material's thermal behavior and stability under the given testing conditions.

3.3 Design of Experiments

The experimental design to examine the impact of key factors on the properties and environmental footprint of hybrid binders. To systematically assess these factors, a 23 + 2(3) + 1 central composite experimental design was adopted in accordance with the surface response methodology. Table 5 presents the experimental factors and their five coded levels -α, -1, 0, +1, and +α which correspond to factorial, axial and central points. The factors included: %VP (with %PC making up the remainder to total 100%), %NS (added relative to the mass of VP), and the molar ratio of NS/CH. The experimental design and subsequent analysis of variance (ANOVA) were performed using the Design Expert software. The experimental design was used to choose the exact values of the parameters, such as percentages and molarity, based on the range of values available in literature for those parameters. These tests were performed in two separate series to investigate the effect thoroughly. In series A, both activator powders were varied in amount, and then based on those results NS/CH was kept constant at 1 and NS percentage was varied in series B. These tests were performed in two separate series to investigate the effect thoroughly. In series A, both activator powders were varied in amount, and then based on those results NS/CH was kept constant at 1 and NS percentage was varied in series B.

Table 6. In the mix designation, the first number indicates %VP, the second %NS, and the third the molar ratio of NS/CH. These designations are used throughout the remainder of this thesis. For instance, S2 (25–6-0.5) refers to a formulation with 25% VP (the remaining 75% being OPC), 6% NS, and an NS/CH ratio of 0.5. All percentages are expressed by weight unless otherwise specified.

Table 5 System design is referred in % weight.

Factors	Levels				
	-α	-1	0	+1	+α
%VP	0	25	50	75	100
%NS	6	8	10	12	14
NS/CH	0.25	0.5	0.75	1	1.25

These tests were performed in two separate series to investigate the effect thoroughly. In series A, both activator powders were varied in amount, and then based on those results NS/CH was kept constant at 1 and NS percentage was varied in series B.

Table 6 Sample mix design

Formulation Number	Formulation nomenclature	VA (%)	PC (%)	NS (%)	NS/CH
S0	Control sample	0	100	0	0
S1	Without activators	25	75	0	0
	SERIES A				
S2	25-6-0.5	25	75	6	0.5
S3	25-8-0.25	25	75	8	0.25
S4	25-10-1	25	75	10	1
S5	25-12-0.75	25	75	12	0.75
S6	25-14-1.25	25	75	14	1.25
S7	50-6-0.75	50	50	6	0.75
S8	50-8-0.5	50	50	8	0.5
S9	50-12-1	50	50	10	1
S10	75-12-1	50	50	12	1
S15	100-12-1	100	100	12	1
	SERIES B				
S11*	25-12-1	25	75	12	1
S12*	25-14-1	25	75	14	1
S13*	25-16-1	25	75	16	1
S14*	25-18-1	25	75	18	1

CHAPTER 4. RESULTS AND DISCUSSION

4.1 Introduction

To evaluate and compare the performance of mortar, the compressive strength results from each test are presented. The tests were performed on cement mortar samples at various ages: 7 days, 28 days, and 90 days. The impact of replacing cement with volcanic ash is analyzed in relation to the corresponding control samples at different testing ages and curing durations. Tests performed on fresh mortar samples included the flow table test to assess workability, as well as initial and final setting time measurements to evaluate the setting behavior of the mixes. Additionally, the concentrations of dissolved silicon, aluminum, and calcium in an alkaline solution, the formation of the gel phase, and the factors influencing these processes were examined using SEM, EDS, XRD, FTIR, and TGA techniques.

4.2 Flow Table Test

This section presents the flow table test results of mixtures with cement replacement contents from 0% to 50% volcanic ash, and the influence of Na_2SO_4 and $Ca(OH)_2$ as activators.

Flow diameters (D) of all the blends are given in Fig. 27

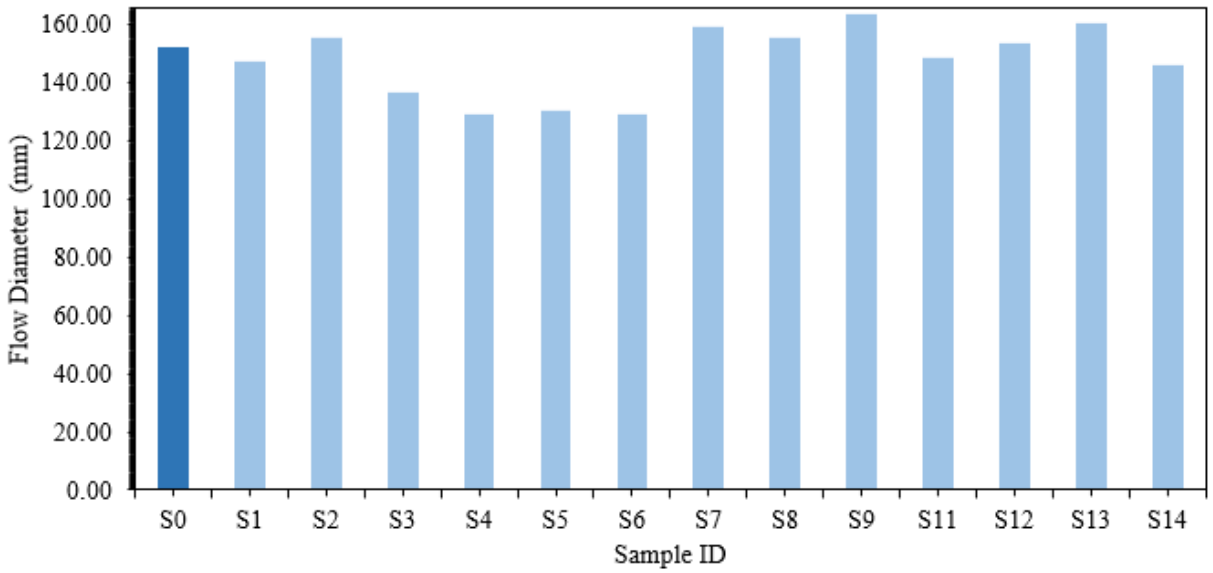

Fig. 27 Flow table diameter spread

The control sample (S0) showed a flow table diameter of 152mm, serving as the baseline for comparison. S1(25-0-0) sample showed a slight reduction in flow diameter (147mm) compared to the

control sample, indicating that the incorporation of volcanic ash without activators marginally reduces workability.

In contrast, sample S2 (25-6-0.25) showed improved flowability (155 mm) compared to the S0. However, samples such as S4 (25-10-1) and S6 (25-14-1.25) exhibited spread diameters of 129mm. This suggests that excessive NS may have a negative impact on the flow properties of the mixture, leading to decreased workability.

Samples with an NS/CH ratio of 1 demonstrated improved flowability compared to those with lower or higher ratios. For instance, S9 (50-12-1) and S13 (25-16-1) recorded the highest flowability of 160 mm and 163 mm, respectively, representing the best performance among all mixtures with 25% and 50% cement replacement respectively.

At 50% cement replacement (S7 (50-6-0.75), S8 (50-8-0.5), S9 (50-12-1)), the flowability remained high as compared to the control sample. The enhanced workability at higher VA replacement levels can be attributed to two key factors. First, the lower water demand associated with VA [64]. Second, the use of chemical activators such as sodium sulfate (Na_2SO_4) and calcium hydroxide ($Ca(OH)_2$) increases the ionic concentration of the mixture [79].

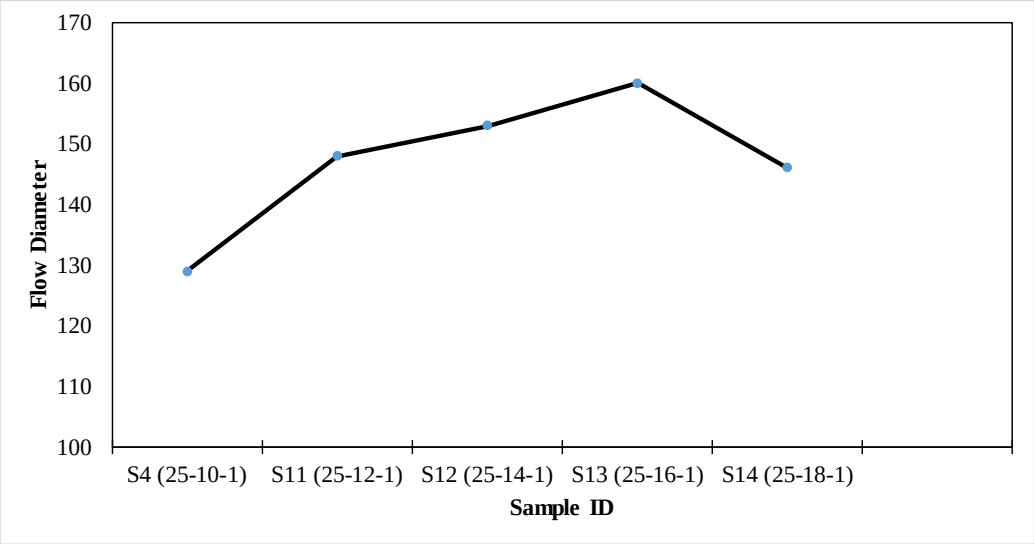

Fig. 28 Effect of NS/CH ratio on flow diameter of pastes with constant VA content (25%)

The results illustrate the influence of increasing NS/CH ratios on flowability**.** As seen in Fig. 29, when the NS/CH ratio increases from 10 (S4) to 16 (S13), the flow diameter improves from 129 mm to a peak of 160 mm, indicating enhanced workability. However, further increasing the ratio to 18 (S14) leads to a slight reduction in flow (146 mm), suggesting that excessively high activator content may affect paste flowability.

4.3 Initial and Final Setting Time Test

Initial and final setting times of the control sample, 25%, and 50% cement replacement are presented in Fig. 29.

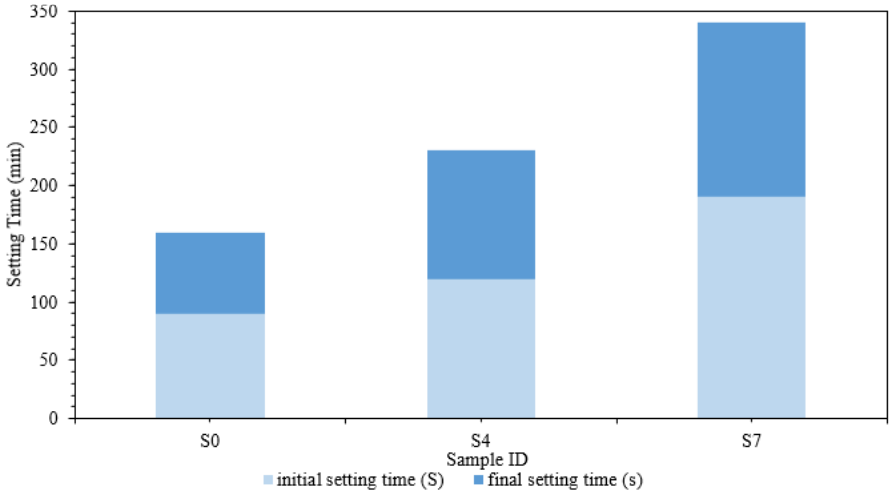

Fig. 29 Initial and final setting time results

The control mix (S0) had initial and final setting times of 90 minutes and 160 minutes, respectively. The incorporation of 25% and 50% VA led to the prolongation of the initial and final setting times to 120/230 and 190/340 minutes respectively, representing increases of 25% and 52% over the control mix.

The introduction of VA into the mix formulation prolonged the setting times of the cementitious mortars, with the influence being more pronounced at the higher replacement level of 50%.

The extension of setting times can be attributed to the reduced reactivity of the binder resulting when OPC is partially replaced by VA [91]. Similar results were reported by Celik et al.[38], who noted that mortars with 30% and 50% cement replacement with VA also had extended setting times.

4.4 Compressive Strength

Fig. 30 illustrates the impact on compressive strength evolution over time with the incorporation of VA and activator powders at varying levels. These tests were performed in two separate series to investigate the effect thoroughly. In series A, both activator powders were varied in amount, and in series B the NS percentage was varied. The data was categorized based on the % of VA. Additionally, reference data was included for comparison, comprising a control of OPC and another set containing OPC blended with a varying proportion of VA without any activators.

Each mixture was mixed with a fixed water-to-cement ratio of 0.48. The results shown are the average of the compressive strength tests completed on four samples for each mixture.

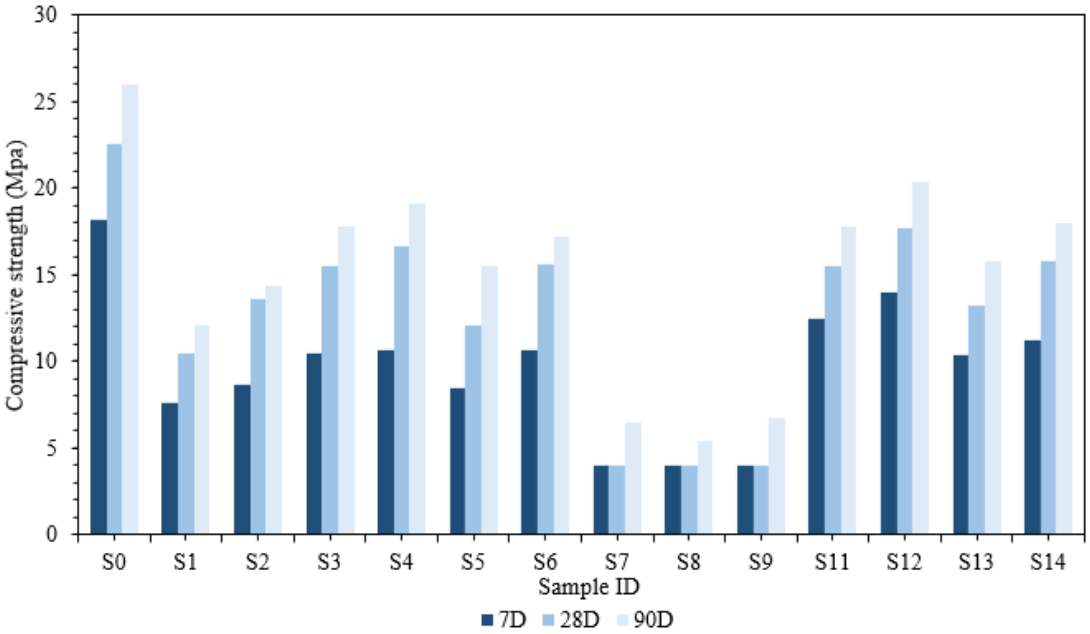

Fig. 30 Compressive strength vs curing days

4.4.1 Series A

The overall compressive strengths of series A at 7-90 days are shown below in Table 7. The reference sample S0 (100% OPC) records higher strengths at all curing ages, ranging between approximately 18-26 MPa from 7-90 days.

Replacement of 25% of the cement by VA without activator powders (S1) resulted in lower compressive strengths (7-12 Mpa) at all ages compared to the control mix (S0). This is anticipated due to the slower pozzolanic reaction of VA [68].

However, the incorporation of NS significantly improved the strength development. The mixes S3 (25-8-0.25) and S6 (25-14-1.25) were particularly effective in this series, with compressive strengths of approximately 16 MPa at 28 days and up to nearly 18 MPa at 90 days. Likewise, S4 (25-10-1) also attained similar strengths at 28 days and demonstrated greater strength at 90 days. This increase underscores the beneficial role of NS in activating the pozzolanic reaction of VA, generating additional C-S-H gel that results in the compressive strength.

Although the additional NS increased the compressive strength, S5 (25-12-0.75) recorded slightly lower 90-day strength 15.5 MPa, compared to the S3 (25-8-0.25), S4 (25-10-1), and S6 (25-14-1.25) samples, which suggests that there may be an optimum range of NS or NS/CH dosage for achieving maximum strength. To confirm and further investigate this optimum dosage, additional tests were conducted by

varying the NS percentage while keeping the NS/CH ratio constant, resulting in an additional set of specimens designated as Series B.

Table 7 Series A compressive strength after 7, 28 and 90 days of curing

Sample ID	Formulation nomenclature	7d Compressive strength (MPa)	28d Compressive strength (MPa)	90d Compressive strength (MPa)
S0	Control Sample	**18.2**	**22.6**	**26.0**
S1	25-0-0	7.6	10.5	12.1
S2	25-6-0.5	8.7	13.6	14.3
S3	25-8-0.25	10.5	15.5	17.8
S4	25-10-1	10.7	16.7	19.2
S5	25-12-0.75	8.4	12.1	15.5
S6	25-14-1.25	10.7	15.6	17.2
S7	50-6-0.75	Less than 10kN	Less than 10kN	6.5
S8	50-8-0.5			5.4
S9	50-12-1			6.7
S10*	75-12-1	(Not suitable for testing)		
S15*	100-12-1			

Increasing the VA replacement ratio to 50% (S7-S9) resulted in a notable decrease in compressive strength, even with the addition of NS. Specifically, S7 (50-6-0.75) exhibited very low early-age strengths and achieved only 6.5 MPa strength at the 90-day point. Similarly, S8 (50-8-0.5) and S9 (50-12-1) also had very low early-age strengths and low 90-day strengths of around 5.4 MPa and 6.7 MPa, respectively. The results indicate that increasing VA content to 50% renders even activated pozzolanic activity inadequate to offset the lowered cement content.

Finally, S10* (75-12-1) and S15* (100-12-1) were not considered suitable for testing as defects were detected, and therefore, it could not be established if these could be reasonably tested for compressive strength.

The lower strength observed in mixers with higher VA content could be attributed to several factors. Firstly, the high volume of VA may lead to a dilution effect [71, 87], reducing the overall cementitious material available for hydration. Secondly, VA typically has a slower pozzolanic reaction compared to OPC, which can delay the formation of C-S-H gel which helps with strength development [28] . Lastly, the particle size and surface area of volcanic ash might affect the packing density [18, 48] and bonding within the mixture, further contributing to the reduced early strength.

4.4.2 Series B

The overall compressive strengths of series B at 7-90 days are given below in the Table. 8. Series B considers mixtures with 25% cement replacement by VA, in which the percentage of NS varies but the ratio NS/CH is maintained constant. This allows us to investigate the influence of the variation of activator dosages on the CS.

Table 8 Series B Compressive strength for 7, 28 and 90 days of curing

Sample ID	Formulation nomenclature	7-d Compressive strength (MPa)	28-d Compressive strength (MPa)	90-d Compressive strength (MPa)
S0	Control Sample	**18.2**	**22.6**	**26.0**
S11	25-12-1	12.4	15.5	17.8
S12	25-14-1	14.0	17.7	20.3
S13	25-16-1	10.4	13.2	15.8
S14	25-18-1	11.2	15.8	18.0

The S12 sample, containing 14% NS, achieved the highest compressive strength at all ages: 14.0MPa at 7 days, 17.7 MPa at 28 days, and 20.3 MPa at 90 days. Although all Series B mixes showed strength gains over time, S12's results indicate that an optimal NS dosage of around 14% leads to comparatively higher strength.

Increasing the NS content beyond this level did not result in further improvements. S13 (25-16-1) and S14 (25-18-1) recorded lower strengths than S12 (25-14-1) at all ages, implying that too much NS might impede strength development, potentially by interfering with C-S-H gel formation or by altering the microstructure. This analysis suggests that while the NS/CH ratio is important, optimizing the NS dosage can lead to significant strength improvements.

Comparison of the best performing samples from series A and B shows:

- Series A: S4 (25-10-1) reached 19.2MPa at 90 days.
- Series B: S12 (25-14-1) reached 20.3MPa at 90 days.

Series B illustrates that a higher NS dosage (14% versus 10% in S4) can enhance performance when the NS/CH ratio remains constant. This emphasizes the need for careful management of both NS dosage and NS/CH ratio to achieve optimal strength development in VA-blended mortar.

To gain a deeper understanding of the hydration phenomena, SEM images and EDS analyses have been utilized. These techniques provide detailed insights into the microstructural characteristics and elemental composition of the mixtures, helping to elucidate the reasons behind the observed variations in compressive strength. The details of these analyses are provided in the following section.

4.5 SEM

SEM was used to examine the influence of partial substitution of OPC with VA on the microstructure of hardened cement paste. The hydration products expected after 28 days of curing are calcium silicate hydrate (C-S-H), calcium hydroxide (C-H), calcium carbonate (CaCO3), and ettringite, as documented in previous research [92, 93].

SEM micrographs reveal variation in the microstructure of the control sample and VA-blended mortars, and the individual phases are easily identified. Needle-shaped ettringite and hexagonal C-H crystals are observed in the control sample. Ettringite is observed dispersed in the control mix but is embedded in C-S-H and C-H in VA-containing samples.

Polished backscattered electron images of the microstructure were characterized based on a gray-scale intensity. The grayscale intensity ranged from 0 (black). Different shades of gray are assigned based on the intensity from 0 to 1 with an interval step of 0.1 [8, 36]. The gray-scale contrast on the image can be physically associated with the interaction of the microstructure with incident X-rays, with the densest solids having the brightest phases where X-rays were adsorbed, and pores represent the darkest phase with little to no interaction with the beam. Unreacted VA are identified by their angular shape and dark gray tone and reacted OPC particles with a bright core (grayscale intensity >0.7) of anhydrous phases relative to the anhydrous phases.

These unreacted particles showed reduced brightness due to the water present in the calcium dominated phases and pores present in the alumina rich phases [94, 95].

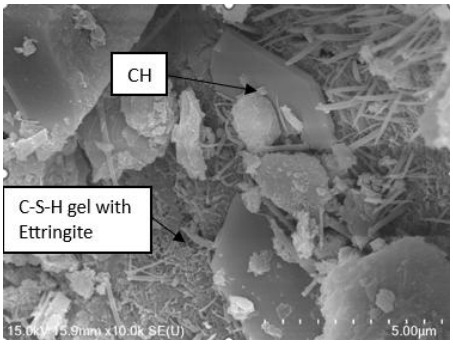

Fig. 35 SEM image of S0

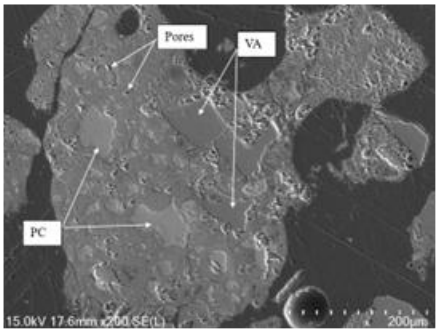

Fig. 34 BSE image of S0

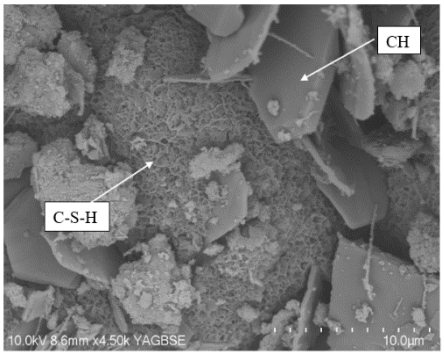

Fig. 31 SEM image of S1

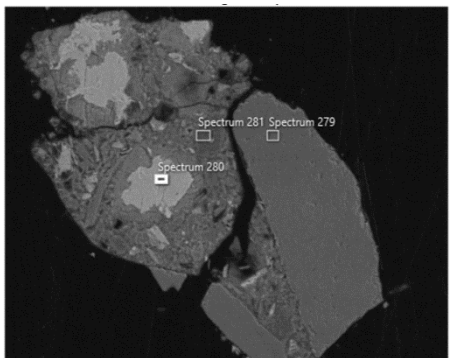

Fig. 32 BSE image of S1

The analysis of sample S1 (25-0-0) (Fig. 322) reveals features through EDS spot analysis. The results show that Spectrum 279 (Fig. 33a) indicates a sample rich in volcanic ash with high silicon and aluminum and with some alkali content. Spectrum 280 (Fig. 33b) indicates C-S-H modified by volcanic ash. Spectrum 281 (Fig. 33c) indicates interactions between the cement matrix and volcanic ash, which show their complex interplay. In accordance with previously published values in the literature [96], the EDS spot analysis shows that C-S-H is formed with a Ca/Si ratio of 3 to 3.7.

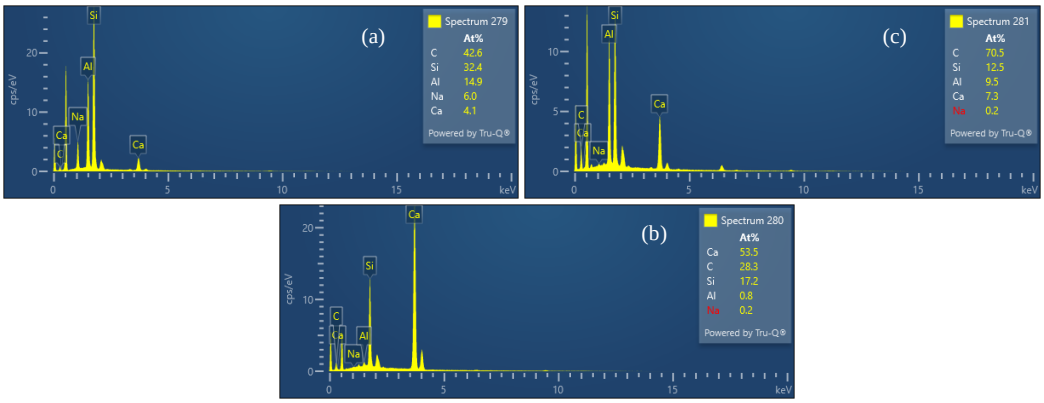

Fig. 33 EDS analysis of S1 sample. (a) - 279 spectrum, (b) - 280 spectrum, (c) - 281 spectrum

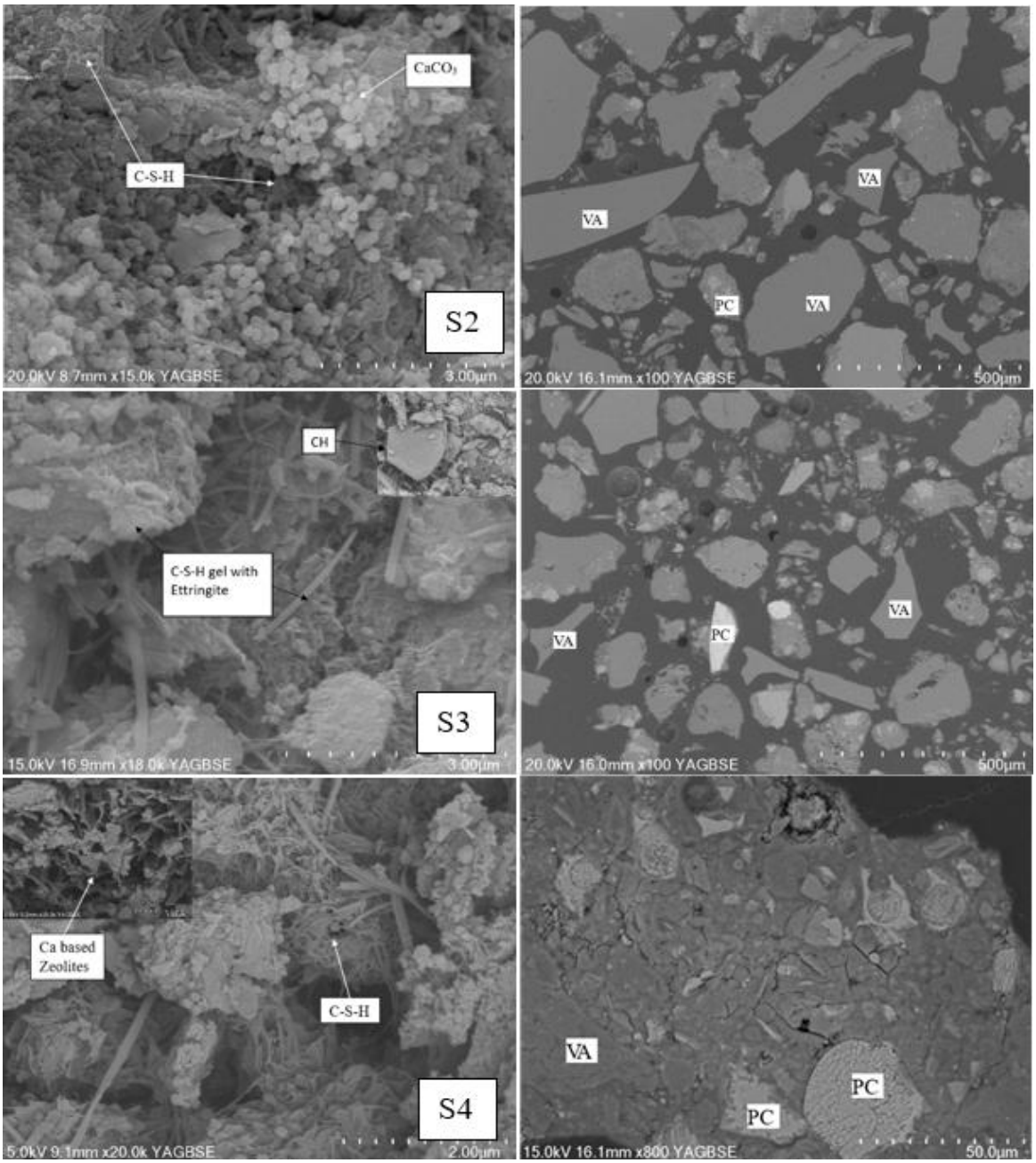

Fig. 36 SEM & BSE images for the samples S2 – S4

SEM and BSE images (Figs. 36 and 37) of samples S2 to S6 show progressive microstructural evolution with increased hydration products and corresponding compressive strength. Samples S4 (25-10-1) and S6 (25-12-1), which recorded higher strengths, displayed denser matrices with abundant C–S–H gel and visible ettringite needles. These mixes showed minimal unreacted volcanic ash (VA) and fewer residual cement particles, indicating enhanced pozzolanic activity. samples S2 (25-6-0.5) and S3 (25 8-0.5) exhibited more unreacted VA particles and less gel formation, correlating with lower mechanical performance. Calcium hydroxide (CH) was less prominent in S4 and S6, suggesting its consumption in secondary reactions. Additionally, S5 (25-10-0.5) showed intermediate features with moderate

hydration product development and scattered zeolite-like crystals that potentially contributed to crack filling and densification.

With the increase of VA content from 0% to 50%, the C─S─H morphology transforms from a gel-type structure to a more compact honeycomb or net-like structure, as previously reported [93, 97].

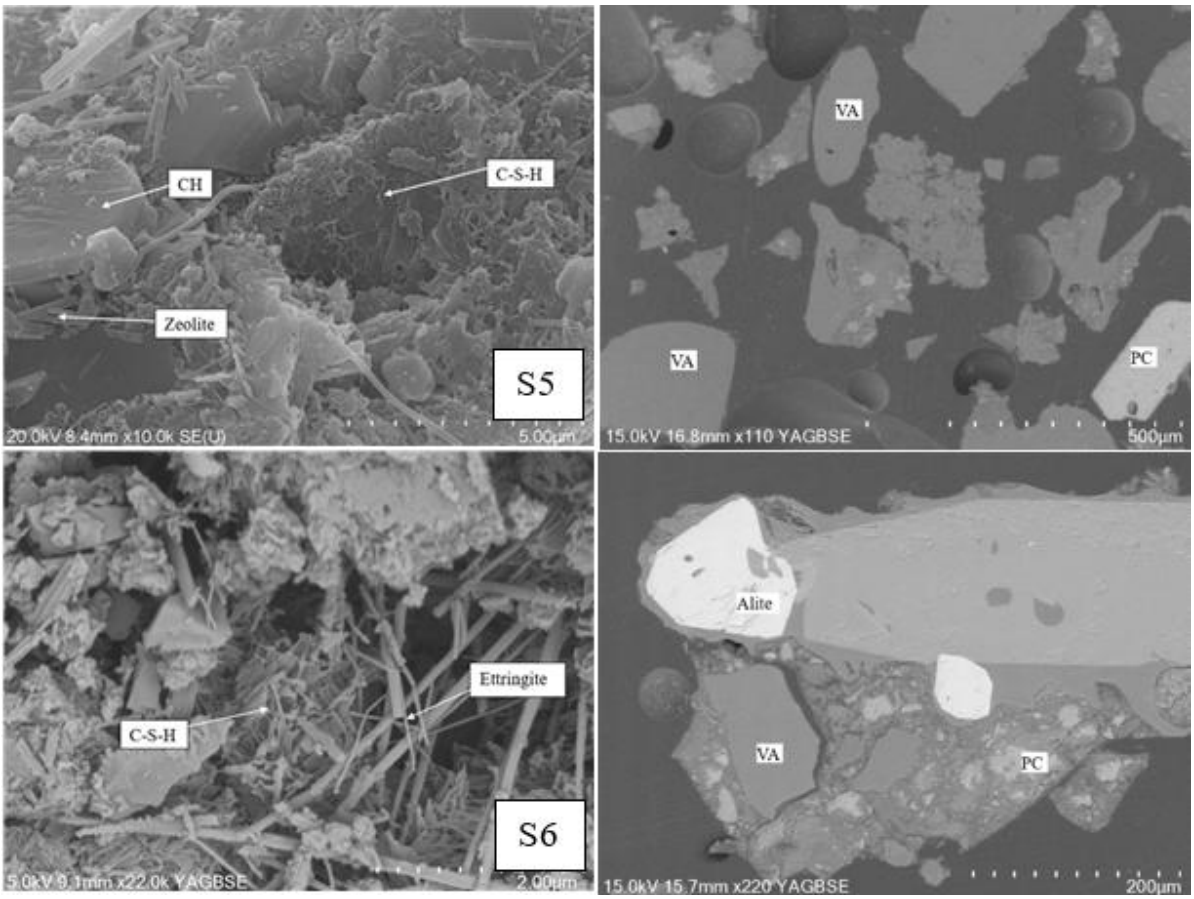

Fig. 37 SEM & BSE images for the samples S5 & S6

With the increase of VA content from 0% to 50%, the C-S-H morphology transforms from a gel-type structure to a more compact honeycomb or net-like structure, as previously reported [93, 97]. These samples exhibited the lowest compressive strength reduction due to the higher microstructure porosity from the high content of VA.

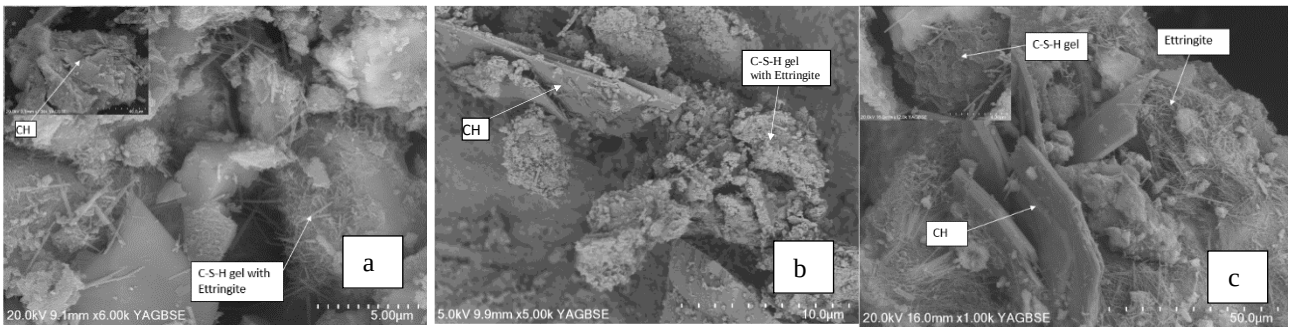

Fig. 38 SEM micrographs of sample (a) S7(50-6-0.75), (b) S8(50-8-0.5) & (c) S9 (50-12-1)

Figures 38 shows the microstructural details of pastes (a) S7 (50-6-0.75), (b) S8 (50-8-0.5), and (c) S9 (50-12-1), revealing abundant C-S-H gel and ettringite alongside visible CH crystals, along with large, unreacted volcanic ash grains and noticeable pore spaces. Compared to lower VA blends, these pastes have less overall gel formation and more residual VA, which corresponds to their lower compressive strengths.

EDS analysis, presented in Fig. 39, indicates that Spectrum 192, obtained from a volcanic ash (VA) region, is characterized by elevated silicon and aluminium concentrations with minimal calcium content, consistent with the composition of rhyolitic VA. In contrast, Spectrum 188, acquired from a distinct, angular particle identified as alite (C_3S), displays a significantly higher calcium concentration with comparatively lower silicon and aluminium levels, confirming its classification as an unhydrated OPC phase. The combined SEM and EDS analyses support the presence of residual precursor materials and a limited extent of hydration in mixtures with high VA content, which correlates with the reduced compressive strength observed in these samples

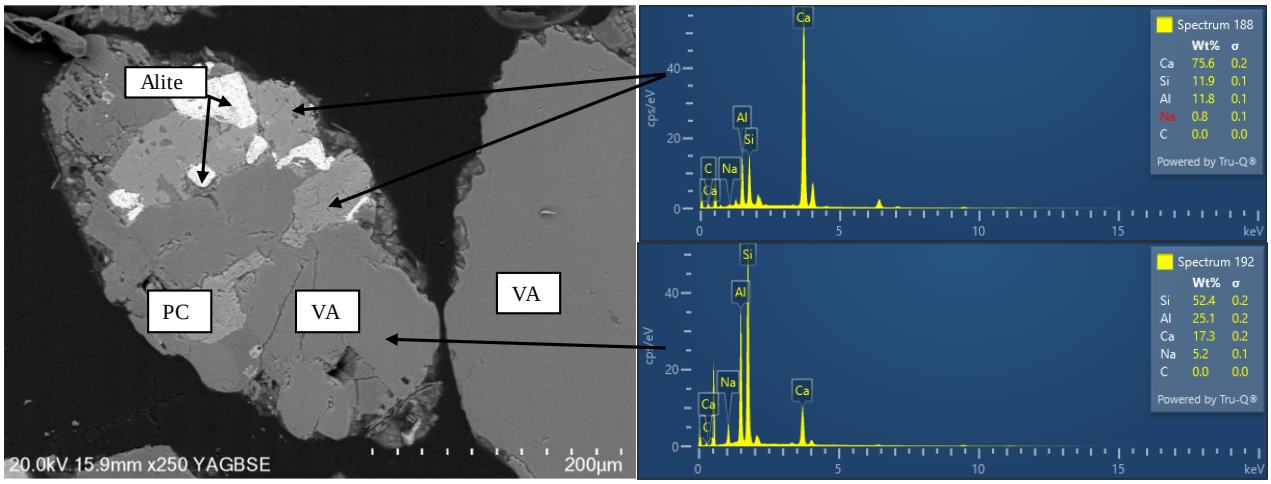

Fig. 39 EDS analysis of sample S7

Within those samples containing high VA content, there were more unreacted VA particles, suggesting a lower degree of reaction. This is a result of the higher incidence of VA and the lower alkalinity due to the low OPC content. A more-densely gel-like C-S-H structure was present with 25% VA substitution, however 50% VA replacement mixtures instead developed a microstructure that is more porous, along with detectable unreacted VA particles.

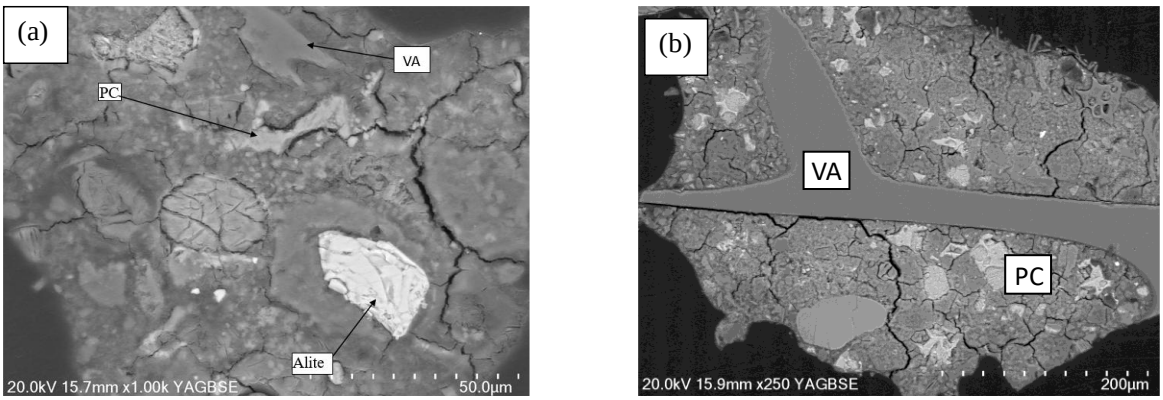

Fig. 40 BSE analysis of (a) S8 (50-8-0.5) & (b) S9 (50-12-1)

Hydration products like C-S-H and CH are also found in sample S11 (25-12-1) (Fig. 41). In these samples the C-S-H gel appeared as a thick, gel-like substance, while the CH crystals appeared as smaller hexagonal shapes when compared to the control sample (S0).

In S12 (25-14-1) (Fig. 41), which produced the highest 28-day compressive strength of 17.675 MPa among the VA-replacement samples, a more refined and interconnected microstructure was noticed. The SEM images reveal a well-distributed C-S-H gel with a honeycomb-like structure, hinting at an enhanced pozzolanic reaction and better matrix densification. The CH crystals were smaller and more evenly distributed, and fine ettringite needles are nestled within the C-S-H matrix. The reduced number of unreacted VA particles suggests a higher level of reaction, which contributes to the improved mechanical properties of this sample.

Samples S13 (25-16-1) and S14 (25-18-1) (Fig. 42) show a more porous microstructure, with a greater number of unreacted VA particles. The CH crystals are present but appear less organized, and the ettringite needles are sparse and not as well integrated into the matrix.

The differences in the morphology of the C-S-H gel, the size of the CH crystals, and the distribution of ettringite has a direct impact on the mechanical performance of the mortar. This result highlights the importance of optimizing the VA content and mix design to achieve the desired material properties.

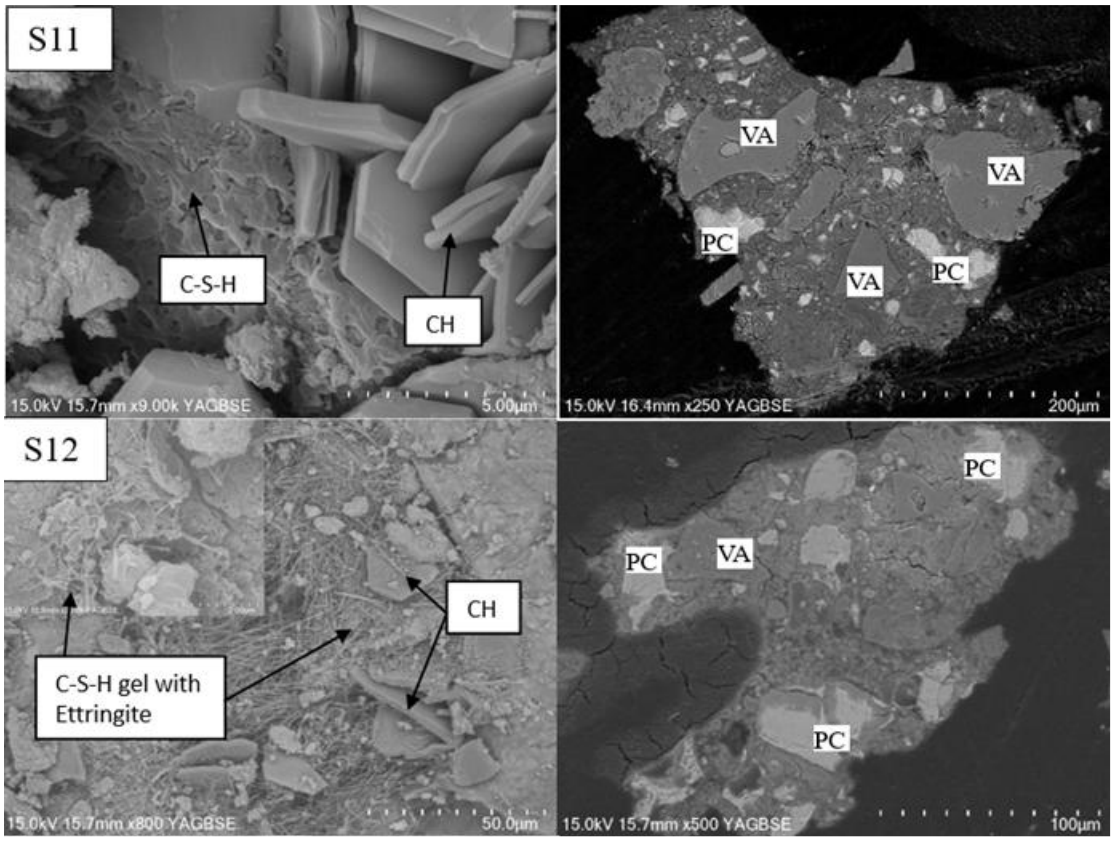

Fig. 41 SEM & BSE images of sample S11, & S12

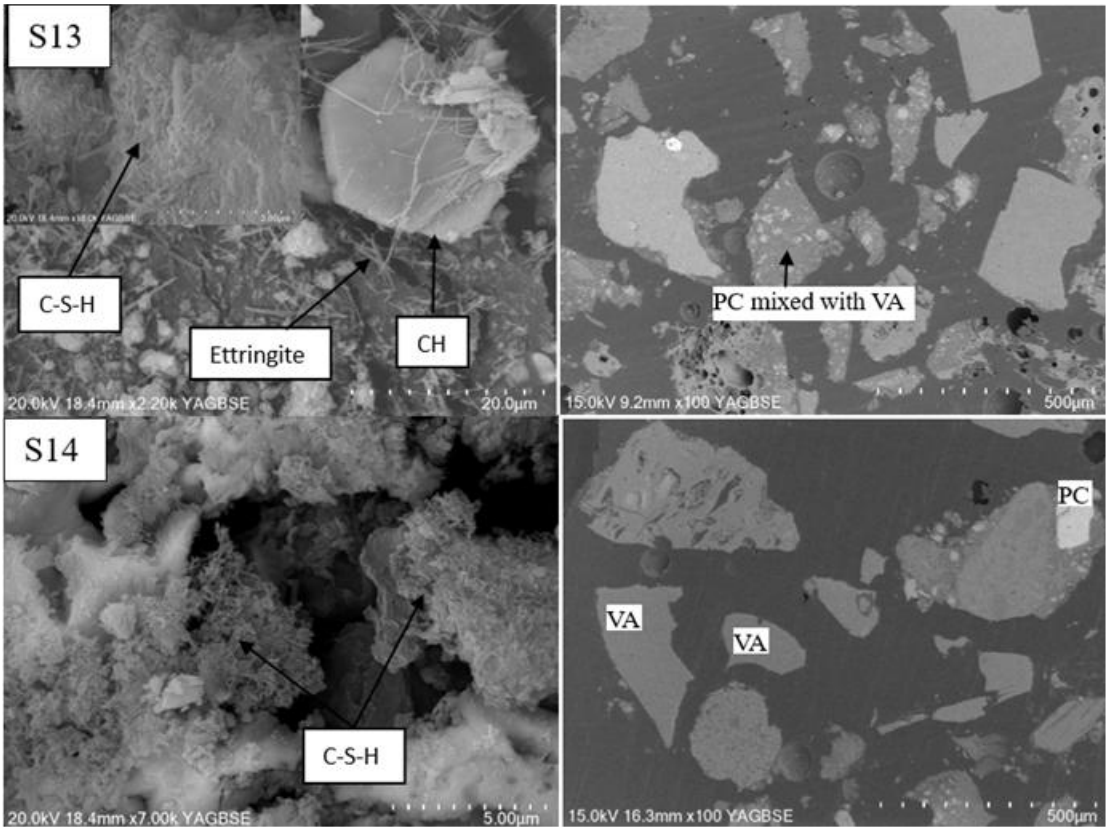

Fig. 42 SEM & BSE images of sample S13, & S14

4.6 FTIR

Fourier Transform Infrared (FTIR) spectroscopy was used to evaluate the hydration and carbonation behaviour of all specimens after 28 days of curing. The results, presented in Fig. 44-46, highlight distinct differences in the intensity and position of absorption bands associated with various hydration and carbonation products.

In the control sample there are no broad bands between wave numbers 4,000 and 3,000 cm^{-1}. These bands are assigned to O-H stretching vibrations, which are associated with calcium hydroxide [92]. The first peak (S0) seen at 2,916 cm^{-1} in Fig. 43 suggests a methylene non-symmetry stretch vibration [98]. The peaks at 2,360 and 2,343 cm^{-1} corresponding to C-O (CO_2) stretching vibrations [99]. The peak at 2,200 cm^{-1} corresponds to C≡C stretching [100], which implies either the presence of alkynes or specific additives. Si-O stretching vibrations around 976 cm^{-1} resemble silicate structures similar to the major C-S-H gel band in the hydrated Portland cement appearing at around 969-970 cm^{-1} [36]. Peaks at lower wavenumber in the S0 and S1 samples appeared at 410 and 422 cm^{-1}. The Si-O-Si vibration of C-S-H was represented by the peaks between 450 and 500 cm^{-1} [36].

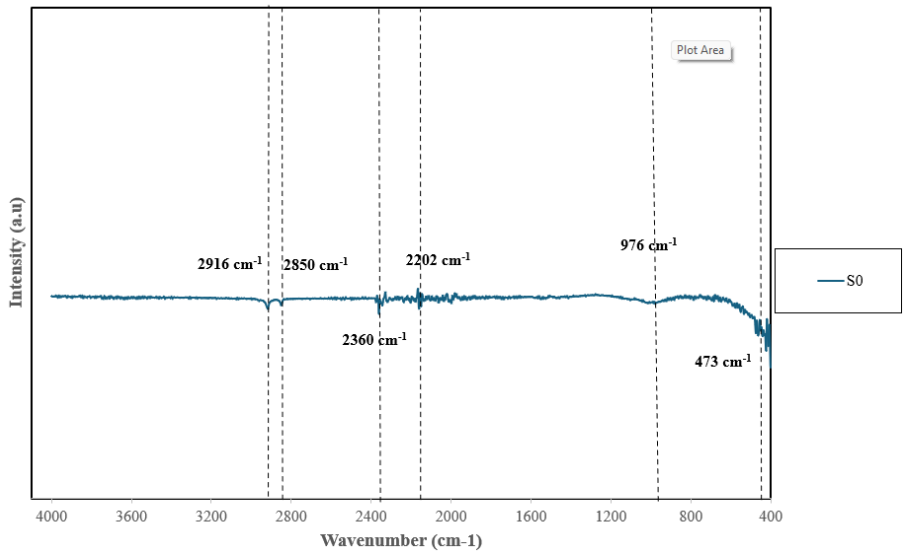

Fig. 43 FT-IR spectra for Cement mortar sample at 28 days

In the samples from S1-S6, prominent peak at 3737.37 cm^{-1} indicates O-H stretching, typical of hydration products such as calcium silicate hydrates (C-S-H) or portlandite [58]. Besides, In S1 C-H stretching vibrations of alkanes can be located at around 2849.31cm^{-1} and 2916.81 cm^{-1}[101], and peaks in the range of 2336-2364 cm^{-1} which are caused by carbonate radical vibrations, indicating the presence of carbonates [102], while the C-O from CO_3^{2-} vibrated at a lower frequency from 1421-1458 cm^{-1} [103]. Si-O stretching vibrations, characteristic of C-S-H gel and silicate network development,

occur between 900 and 1100 cm^{-1} in all samples, and Si-O-Si vibrations are also revealed by peaks between 450 and 500 cm^{-1} [104]. S2 shows intense silicate presence (1037 cm^{-1}, Si-O stretching) with extensive carbonation (1488, 1508, and 1647 cm^{-1}, O-H bending)[104].

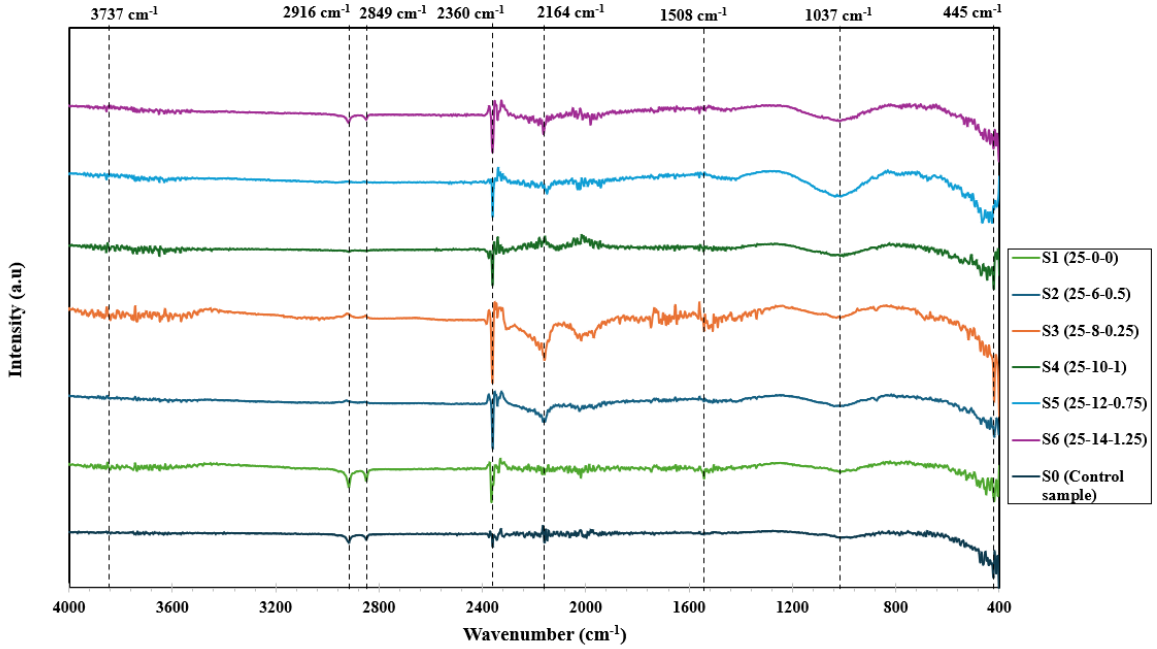

Fig. 44 FT-IR spectra for Series A 25% VA sample at 28 days

S3 has a more intense carbonate peak (1488 cm^{-1}) but possibly less activator interaction. S4 has a distinctive peak at 2038 cm^{-1}, similarly S5 has a distinctive peak at 2150 cm^{-1}, with peaks in the 2000-3000 cm^{-1} range might be due to vibrations like C-H of hydrocarbons [103]. In sample S4 has peaks at 1542 cm^{-1}, corresponding to the bending vibration of unbound water molecules which have wave at 1500^{-1}-1700 cm^{-1} [103].

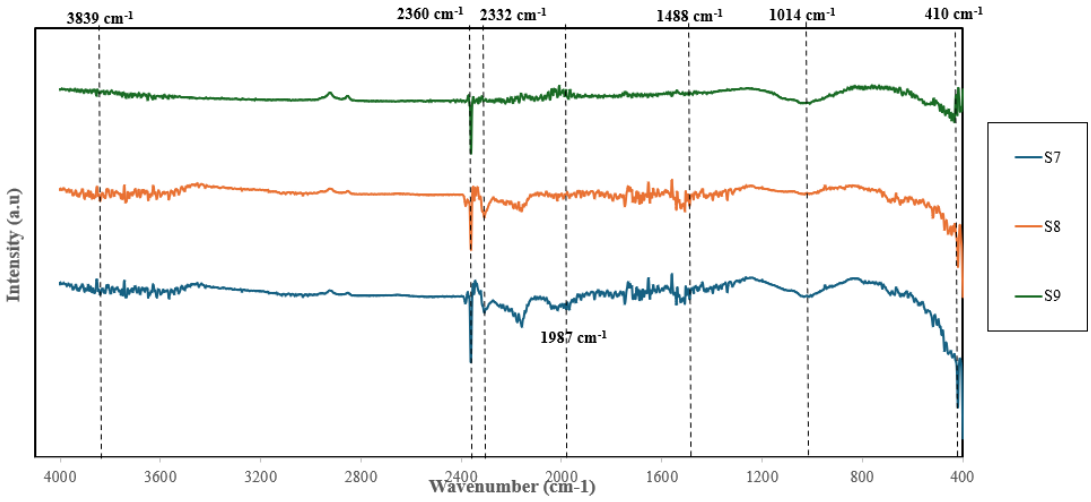

Fig. 45 FT-IR spectra for Series A 50% VA sample at 28 days

FTIR spectra of 50% volcanic ash replacement cement mortar samples (S7, S8, S9) (Fig. 45) reveal valuable structural and chemical information. Broad O-H stretching vibrations (3500-4000 cm^{-1}) [98] and Si-O stretching (1000-1032 cm^{-1}) [104] peaks confirm the presence of hydration products such as C-S-H gel and silicate networks, which are key to strength. However, the lower intensity of silicate peaks compared to 25% replacement samples shows a less mature network, which may be the cause of the lower compressive strength. Intense carbonate vibrations (1488-1508 cm^{-1}) are indicative of active carbonation [104], which, while beneficial at early stages, can preclude long-term strength by consuming reactive phases. Characteristic peaks in S9 (1972-1987 cm^{-1}) suggest presence of intermediate phases. These findings demonstrate the trade-offs within high-replacement mortar blends and show the need to optimize volcanic ash content for balanced performance and sustainability.

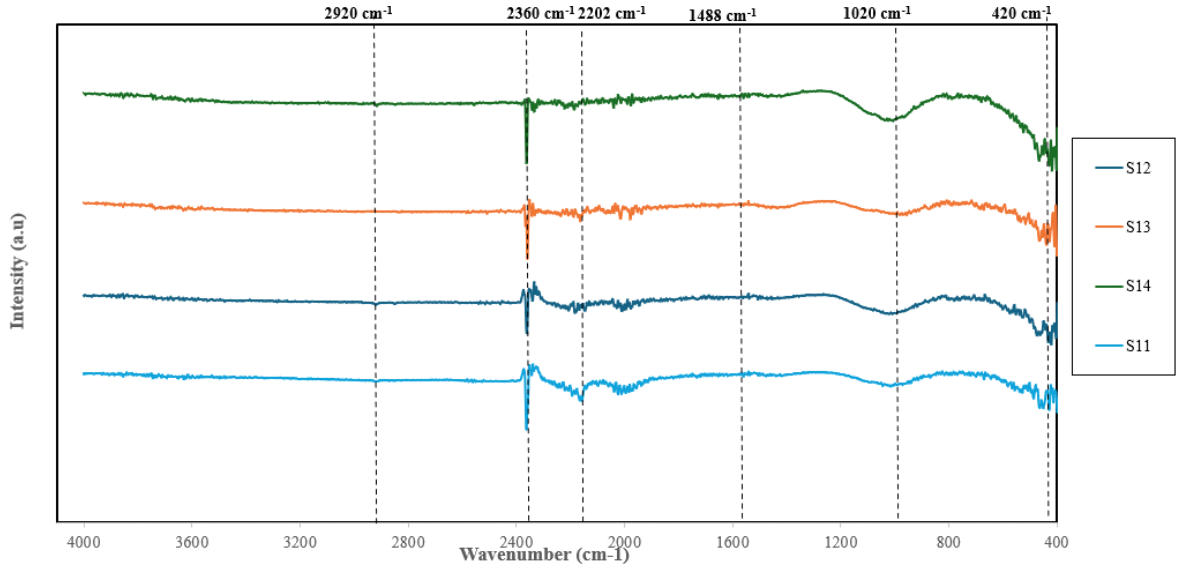

Fig. 46 FT-IR spectra for Series B 25% VA sample at 28 days

FTIR spectra of samples S12-S14 (Fig. 46) show similar Si-O stretching peaks near 1000-1021 cm^{-1}, which shows the formation of silicate networks that are responsible for mortar strength. The sulphate vibrations at 670-604 cm^{-1} indicate the significant role of sodium sulphate in the mixture. Peaks in the range of 2000-2040 cm^{-1} show the existence of specific interactions between volcanic ash and activators, which could influence material properties. The typical appearance of peaks for carbonate or CO_2 at about 2360 cm^{-1} shows that the carbonation reactions in the mixtures. This may influence mortar performance over time. There are no broad absorption bands between 4,000 and 3,000 cm^{-1} similar to the S0 sample. The above results demonstrate the complicated chemical interaction in VA replacement mixtures under the influence of different sodium sulphate contents without keeping the NS/CH ratio constant.

The asymmetric Si–O–Si stretching vibration peak at 976 cm^{-1} in the control sample shifted to 1037 cm^{-1}, 1014 cm^{-1}, and 1020 cm^{-1}, while its bending vibration shifted from 473 cm^{-1} to 445 cm^{-1}, 410 cm^{-1}, and 420 cm^{-1} respectively, in the Series A (25% and 50% VA replacement) and Series B (25% VA) samples. These shifts to higher wavenumbers indicate increased polymerization and incorporation of aluminium into the silicate structure, reflecting the formation of calcium aluminosilicate hydrate (C-A-S-H) gel as a result of the pozzolanic reaction between volcanic ash and calcium hydroxide [105].

4.7 XRD

The XRD analysis provides detailed information on the hydration reaction in the control and VA replacement samples after 28 days of curing (Fig. 47-49).

Fig. 47, the intensity of the characteristic peak for calcium hydroxide (Portlandite) seen at a 2θ angle of 18.01° is lower in the samples (S1-S6) compared to the control sample. These samples exhibited better gel formation, as supported by the FTIR and SEM results.

There is an amorphous halo between 20° and 35° 2θ, which was less intense and shifted towards greater angles in all reacted VA replacement mixtures. This suggests that the vitreous phase of VA has reacted, forming amorphous cementitious reaction products that have contributed to the strength development [106].

All reacted 25% VA replacement mixtures from Series A showed quartz (~20.7, ~26.6) and dolomite (~24.3°, 29.5°, 35.97° 2θ) signals from the unreacted VA [15], while the signals from the reaction products included C-S-H (overlapping with the calcite peak at ~29.3°, 29.4°, and 29.5° 2θ) [21] and C-A-S-H gel (Gismondine (~27.7, 27.9 2θ) [15].

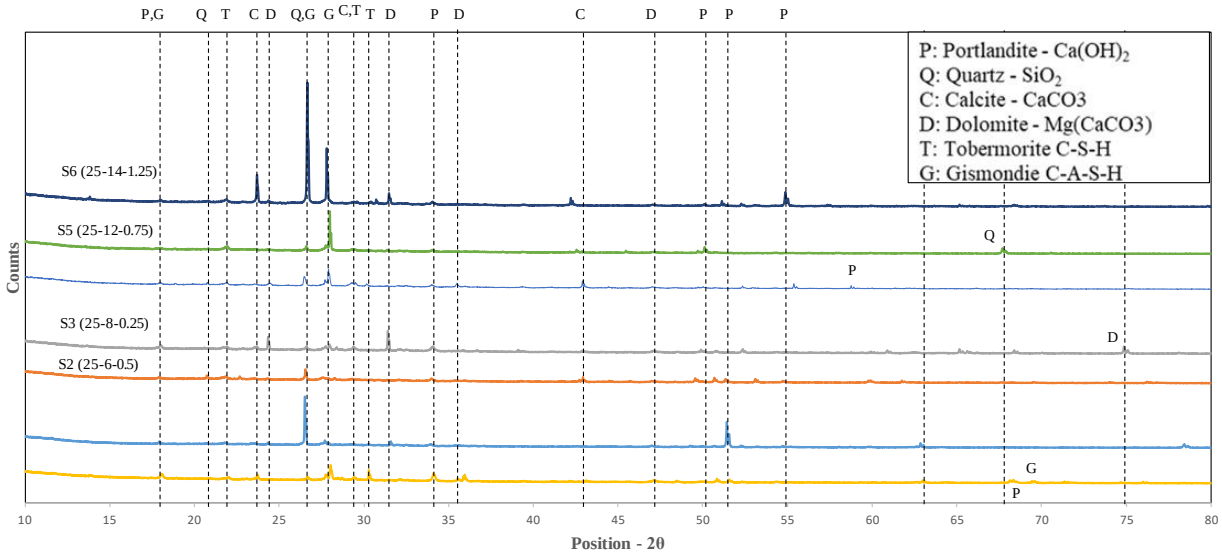

Fig. 47 XRD patterns for Series A 25% VA sample at 28 days

The XRD patterns of the mixtures containing 50% VA, shown in Fig. 48, exhibit distinct peaks for portlandite at approximately 2θ = 18.0°, 34.1°, and 47.2°, which are attributed to calcium hydroxide generated from the hydration of OPC and, potentially, from unreacted $Ca(OH)_2$ added as a chemical activator [28]. In general, the mixtures with 50% VA replacement showed similar features across all samples. The main reaction product is an amorphous C-S-H gel, which is likely intermixed with crystalline phases such as portlandite and calcite. Complementary observations from SEM micrographs (Fig. 38) confirm the intermixing of C-S-H gel with needle-like ettringite, and the presence of ettringite was further supported by identifiable peaks in the XRD spectra.

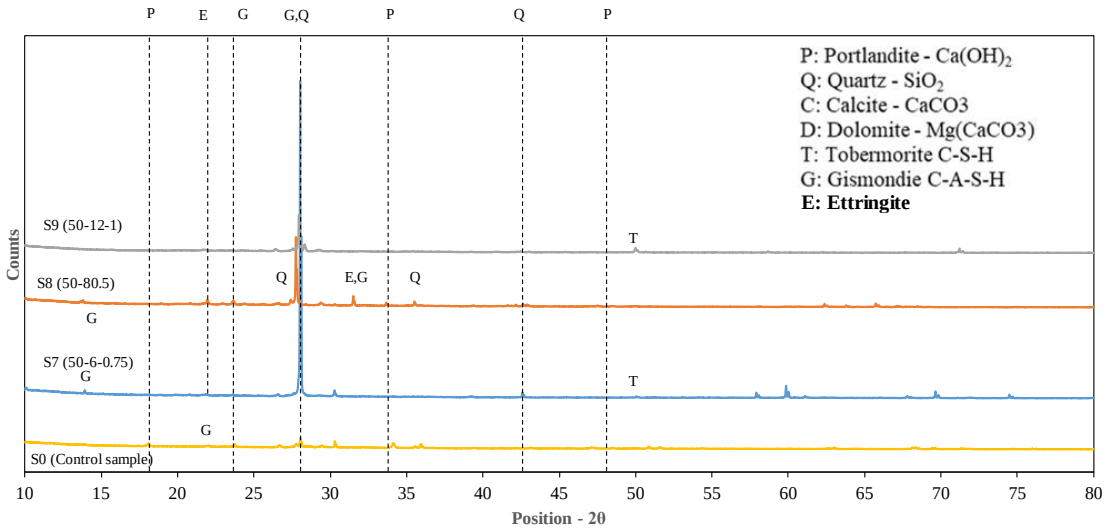

Fig. 48 XRD patterns for Series A 50% VA sample at 28 days

The XRD Peaks of pastes with 25% VA replacement (Series B) are shown in the Fig. 50.

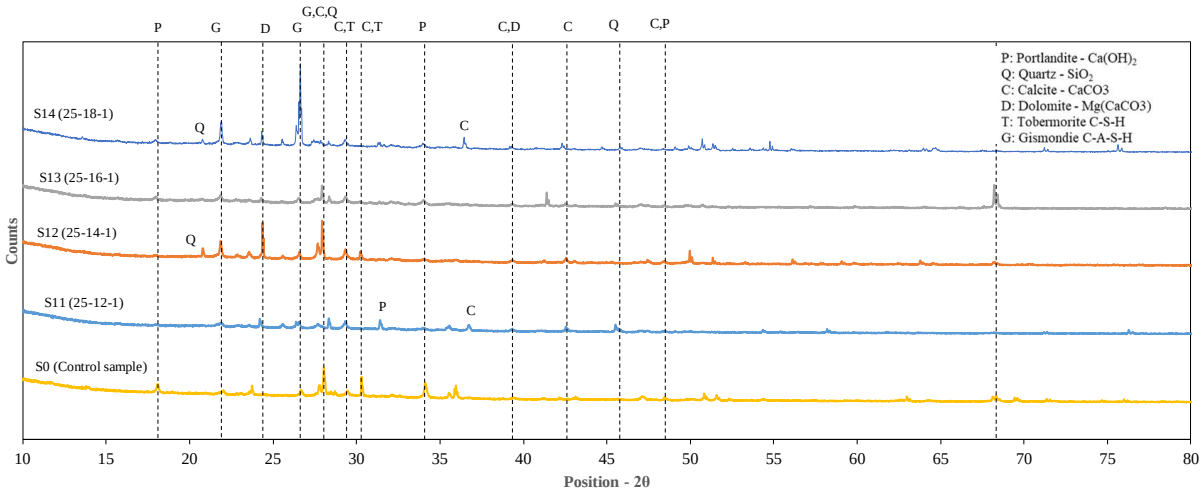

Fig. 49 XRD patterns for Series B 25% VA sample at 28 days

A notable trend observed across this series is the progressive reduction in portlandite intensity with increasing activator dosage. In particular, portlandite peaks, most clearly visible in S11, diminish substantially in S12 and become nearly undetectable in S13 and S14. C-S-H formation is confirmed by the presence of peaks at peaks at ~17.9°, 34.4° and 47.01° 2θ [107]. These features appear alongside and intensified peaks assigned to Gismondine (C-A-S-H) and Calcite (CaCO3) in the 2θ range of ~26.62° [36] to 29.32° [15] are evident in the higher-activated pastes (S13 and S14). The peak near ~ 29.34° 2θ indicates the development of crystalline hydration products such as Tobermorite [108]. These phases are indicative of the formation of well-crystallized hydration gels. Quartz in the 2θ range of ~20.7°, ~26.5°, ~39.3° to 42.5° [15, 109] persists across all samples due to unreacted siliceous components inherent in the volcanic ash.

4.8 TG-DTG

TGA curves give the weight changes of samples due to heating, while DTG curves give the rate of change of weight (or the first derivative of the TG curve). By using these curves, the weight losses due to transitions can be computed.

Selected mortar samples (S0, S4, S9, and S12) based on their compressive strength performance, were subjected to thermogravimetric analysis (TGA) and derivative thermogravimetry (DTG) in order to examine the stability of hydration products.

Different researchers use different methods to calculate weight losses due to desorption, dehydration, dehydroxylation and decarbonation. The temperature ranges considered by various authors are shown in the Table 9 and indicated some similarity.

Table 9 Temperature ranges considered by various authors

	Desorption	Dehydration	Dehydroxylation	Decarbonation
EI Jazira and Illston [110]	30-105 ºC	105-440 ºC	440-580 ºC	580-1007 ºC
Vedalakshmi et al. [111]	30-100 ºC	100-300 ºC	300-350 ºC	450-700 ºC
Monteagudo et al. [112]	30-105 ºC	105-430 ºC	430-530 ºC	530-110 ºC
Bhatty [113]	30-105 ºC	105-440 ºC	440-580 ºC	580-1100 ºC

The literature implies that it is common practice to select ranges based on the nature of the curves obtained. Accordingly, by considering all the TGA-DTG curves of this research, the following temperature ranges were developed on to compute weight losses.

30 - 100 °C	Desorption
100 - 420 °C	Dehydration
420 - 550 °C	Dehydroxylation
550 – 800 °C	Decarbonation

The range determined for desorption was set to 30 - 100 °C thus, it was assumed that the free water in the sample completely removed when the test surpasses 100 ºC.

All mixes exhibit a mass loss around 30-100 °C from free-water desorption. S4, which incorporated 25% VA and a 10% Na_2SO_4 dosage, showed the highest initial mass loss (5.44%) in the desorption region. S9 characterized by a higher VA content (50%) exhibited the lowest initial water loss (2.64%). Bound water loss from C-S-H is associated with the 100-420 °C range, with S0 and S9 showing the highest mass losses (3.86% and 3.47%, respectively), indicating a more extensive formation of traditional hydration gels. S4 and S12 exhibit markedly lower dehydration losses (1.99% and 1.87%). The dehydroxylation step (420-550 °C) highlights variations in portlandite consumption among mixtures. S12, with the smallest loss (0.65%), has effectively consumed $Ca(OH)_2$ through pozzolanic conversion, while S4 and S9 retain higher CH fractions (~1.09% and 1.06%), and the control mix S0 falls in between (0.96%). This pattern suggests that S12 experienced the most effective pozzolanic reaction among the tested samples, correlating with its enhanced gel formation and superior strength performance. In the decarbonation range (550-800 °C), mass loss trends further illustrate differences in matrix densification and carbonation susceptibility. S4 shows the highest loss (3.02%), likely due to excess unreacted CH and an open pore structure facilitating CO_2 ingress. S9 follows at 2.48%, while S0 (2.00%) and the dense, well-reacted S12 carbonate shows the least loss of mass (1.93%)

Table 10 Mass loss values in temperature ranges

Temperature range (ºC)	Mass loss values (%)			
	S0	S4	S9	S12
30-100	4.27	5.44	2.64	3.69
100-420	3.86	1.99	3.47	1.87
420-550	0.96	1.09	1.06	0.65
550-800	2	3.02	2.48	1.93

Table 11 Peaks of the DTG curves

Temperature range (ºC)	Peak Temperature (ºC)			
	S0	S4	S9	S12
30-100	50.4	71.2	70.6	63.8
100-420	413.2	412.8	293.1	413.9
420-550	459	540.3	462.2	548.8
550-800	664.7	683.1	798.1	687.5

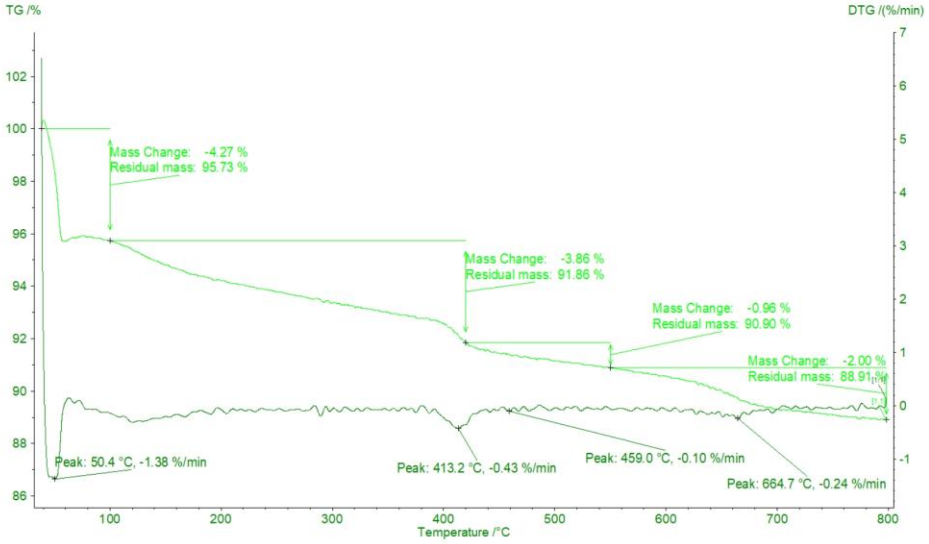

Fig. 50 TG and DTG curves of S0 (control sample) curing at 28 days

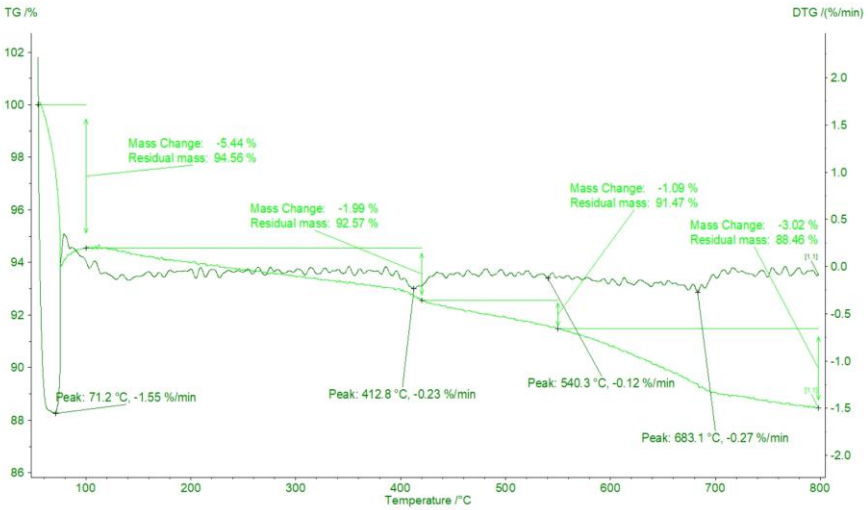

Fig. 51 TG and DTG curves of S4 (25-10-1) curing at 28 days

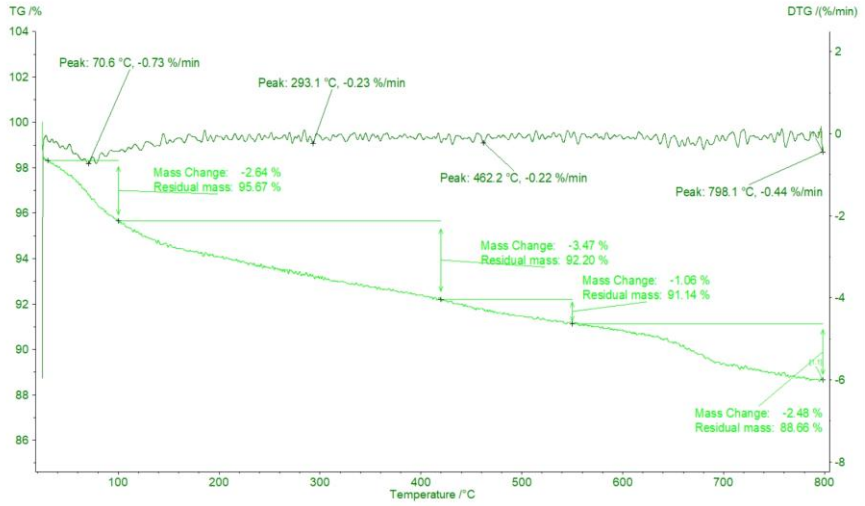

Fig. 52 TG and DTG curves of S9 (50-12-1) curing at 28 days

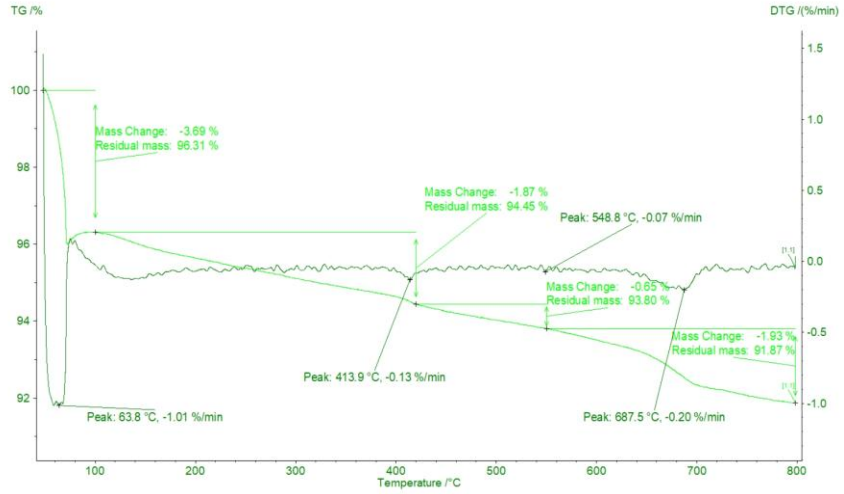

Fig. 53 TG and DTG curves of S12 (25-14-1) curing at 28 days

CHAPTER 5. CONCLUSION & FUTURE STUDY

5.1 Conclusion

This research investigated the feasibility of volcanic ash (VA) as a partial replacement of cement in hybrid mortar systems activated by sodium sulfate (Na_2SO_4) and calcium hydroxide ($Ca(OH)_2$). Although the intention of the research was to enhance sustainability and lower CO_2 emissions by developing a sustainable concrete alternative, the mechanical properties, particularly compressive strength, remained generally inferior to the control OPC sample. Nevertheless, there are some compositions that provide encouraging enhancements, particularly if an optimum dosage of activators is utilized.

- Among all tested mixtures, S4 (25-10-1) from Series A and S12 (25-14-1) from Series B yielded the most promising results. Individually, S4, which contains 25% VA substituted by 10% Na_2SO_4 and an NS/CH ratio of 1, demonstrated higher compressive strength among Series A samples. Meanwhile, S12, with 25% VA, 14% Na_2SO_4, and also an NS/CH ratio of 1, performed better than all other samples in Series A and B, rendering it the most effective hybrid binder composition in this research.
- SEM micrographs of S4 and S12 displayed denser and finer microstructure, more compact C S-H gel networks, and less CH crystals and ettringite needles compared to less optimized mixtures. Such structural improvements indicate effective pozzolanic reaction and are consistent with the higher compressive strength findings.
- FTIR spectra showed the formation of additional silicate and aluminate phases in the optimum mixes, with a shift in absorption bands for Si–O and Al–O bonds. This shows ongoing formation of C-A-S-H and C-S-H phases.
- TGA analysis supported these findings by showing a reduced mass loss within the CH decomposition temperature range (around 400–500°C) for the optimized samples, indicating an improved pozzolanic consumption of calcium hydroxide.

Though the overall performance of the VA-replacement mortars was poor than the control for early compressive strength, these optimized mixtures (S4 and S12) have long term performance. 4 (25-10-1) achieved a 90-day strength of 19.2 MPa, while S12 (25-14-1) reached 20.3 MPa, both of which are significant improvements over S1 (25-0-0), which only reached 12.1 MPa. However, higher percentages of VA replacement negatively influence performance through dilution of the cementitious materials and reduced hydration efficiency. Future research may explore the long-term durability of 60

VA-modified mortar and examine its performance under various environmental conditions, thereby providing additional evidence for its use in sustainable construction.

5.2 Future Study

- Investigate the possibility of high temperature curing (e.g., 40–60°C) to accelerate the pozzolanic reaction of volcanic ash and to improve early-age strength at high percentages of volcanic ash substitution.
- Extend the research to investigate durability parameters like chloride ion penetration, sulfate attack resistance, carbonation depth, and freeze-thaw performance in improved VA-activated systems.
- Assess the synergistic effects of mixing Na_2SO_4 with other activators (e.g., Na_2SiO_3, NaOH, or $CaCl_2$) to improve reactivity and further improve early age strength development.
- Transition from mortar to full concrete mixes, with coarse aggregates, is an effort to evaluate mechanical properties and durability performance in realistic field conditions.
- Investigate more deeply the influence of grinding time and grind fineness on reactivity and strength performance, to establish cost-effective processing pathways.

REFERENCES

1. Scrivener, K.L., V.M. John, and E.M. Gartner, *Eco-efficient cements: Potential economically viable solutions for a low-CO2 cement-based materials industry.* Cement and concrete Research, 2018. 114: p. 2-26.

2. Worrell, E., et al., *Carbon dioxide emissions from the global cement industry.* Annual review of energy and the environment, 2001. 26(1): p. 303-329.

3. Shahjalal, M., et al. *Study on Partial Replacement of Cement with Limonite in Mechanical Strength of Mortar*. in *International Conference on Sustainable Civil Engineering Structures and Construction Materials*. 2020. Springer.

4. Agboola, S., et al., *Effect of Volcanic Ash as Partial Replacement of Cement in Concrete Subject to Aggressive Chemical Environment.* International Journal of Engineering Applied Sciences and Technology (IJEAST), 2021. 6(5): p. 100-108.

5. Hossain, K.M.A., *High strength blended cement concrete incorporating volcanic ash: Performance at high temperatures.* Cement and Concrete Composites, 2006. 28(6): p. 535-545.

6. Moon, J., et al., *Characterization of natural pozzolan-based geopolymeric binders.* Cement and Concrete Composites, 2014. 53: p. 97-104.

7. Játiva, A. and M. Etxeberria, *Exploring the utilization of activated volcanic ash as a substitute for Portland cement in mortar formulation: A thorough experimental investigation.* Materials, 2024. 17(5): p. 1123.

8. Lopez-Salas, J. and J.I. Escalante-Garcia, *Hybrid binders based on volcanic pumice: Effect of the chemical composition on strength and microstructures.* Cement and Concrete Research, 2024. 176.

9. Hossain, M.U., et al., *Designing sustainable concrete mixes with potentially alternative binder systems: Multicriteria decision making process.* Journal of Building Engineering, 2022. 45: p. 103587.

10. Mason, B.J., *The analysis of taupo pumice as an effective partial cement replacement in concrete.* 2012.

11. *<tauranga volcanic ash.pdf>.*

12. Pullar, W., *Volcanic ash beds in the Waikato district.* Earth Science Journal 1967.

13. Kennerley, R.A. and J. Clelland, *An investigation of New Zealand pozzolans*. 1959: Government Printer.

14. Játiva, A., E. Ruales, and M. Etxeberria, *Volcanic Ash as a Sustainable Binder Material: An Extensive Review.* Materials, 2021. **14**(5): p. 1302.

15. Bawab, J., et al., *Synergetic impact of volcanic ash and calcium carbide residue on the properties and microstructure of cementitious composites.* Construction and Building Materials, 2024. **439**: p. 137390.

16. Hossain, M.U., Y. Dong, and S.T. Ng, *Influence of supplementary cementitious materials in sustainability performance of concrete industry: A case study in Hong Kong.* Case Studies in Construction Materials, 2021. **15**: p. e00659.

17. Hossain, M.U., et al., *Sustainable natural pozzolana concrete–A comparative study on its environmental performance against concretes with other industrial by-products.* Construction and Building Materials, 2021. **270**: p. 121429.

18. Celik, K., et al., *High-volume natural volcanic pozzolan and limestone powder as partial replacements for portland cement in self-compacting and sustainable concrete.* Cement and concrete composites, 2014. **45**: p. 136-147.

19. Belayutham, S., et al., *Proceedings of the 5th International Conference on Sustainable Civil Engineering Structures and Construction Materials: SCESCM 2020*. Vol. 215. 2022: Springer Nature.

20. Giergiczny, Z., et al., *Performance of concrete with low CO2 emission.* Energies, 2020. **13**(17): p. 4328.

21. Kupwade-Patil, K., et al., *Impact of Embodied Energy on materials/buildings with partial replacement of ordinary Portland Cement (OPC) by natural Pozzolanic Volcanic Ash.* Journal of cleaner production, 2018. **177**: p. 547-554.

22. Kantarcı, F., I. Türkmen, and E. Ekinci, *Optimization of production parameters of geopolymer mortar and concrete: A comprehensive experimental study.* Construction and Building Materials, 2019. **228**: p. 116770.

23. Alqarni, A.S., *A comprehensive review on properties of sustainable concrete using volcanic pumice powder ash as a supplementary cementitious material.* Construction and Building Materials, 2022. **323**: p. 126533.

24. Kılıç, A. and Z. Sertabipoğlu, *Effect of heat treatment on pozzolanic activity of volcanic pumice used as cementitious material.* Cement and Concrete Composites, 2015. **57**: p. 128-132.

25. Hamidi, M., et al., *Evaluation and improvement of pozzolanic activity of andesite for its use in eco-efficient cement.* Construction and Building Materials, 2013. **47**: p. 1268-1277.

26. Zeyad, A.M., B.A. Tayeh, and M.O. Yusuf, *Strength and transport characteristics of volcanic pumice powder based high strength concrete.* Construction and Building Materials, 2019. 216: p. 314-324.

27. Haddad, R.H. and O. Alshbuol, *Production of geopolymer concrete using natural pozzolan: A parametric study.* Construction and Building Materials, 2016. 114: p. 699-707.

28. Hossain, K.M.A., *Volcanic ash and pumice as cement additives: pozzolanic, alkali-silica reaction and autoclave expansion characteristics.* Cement and Concrete Research, 2005. 35(6): p. 1141-1144.

29. Cai, G., et al., *Volcano-related materials in concretes: a comprehensive review.* Environmental Science and Pollution Research, 2016. 23(8): p. 7220-7243.

30. Kabay, N., et al., *Properties of concrete with pumice powder and fly ash as cement replacement materials.* Construction and Building Materials, 2015. 85: p. 1-8.

31. Susanti, R.D., et al., *Studies on concrete by partial replacement of cement with volcanic ash.* Journal of Applied Engineering Science, 2018. 16(2).

32. Abdulazeez, A.S., et al., *Strength performance of concrete produced with volcanic ash as partial replacement of cement.* International Journal of Engineering Research and Technology (IJERT), 2020. 9(03).

33. Hazarika, A., et al., *Characterization, activation and reactivity – A case study of Nordic volcanic materials for application as Supplementary Cementitious Materials.* Case Studies in Construction Materials, 2025. 22: p. e04096.

34. Shahjalal, M., et al. *Effect of Partial Replacement of Cement with Volcanic Ash on Mechanical Behaviour of Mortar*. in *International Conference on Sustainable Civil Engineering Structures and Construction Materials*. 2020. Springer.

35. Al-Fadala, S., et al., *Significance of performance based specifications in the qualification and characterization of blended cement using volcanic ash.* Construction and Building Materials, 2017. 144: p. 532-540.

36. Kupwade-Patil, K., et al., *Use of silica fume and natural volcanic ash as a replacement to Portland cement: Micro and pore structural investigation using NMR, XRD, FTIR and X-ray microtomography.* Construction and Building Materials, 2018. 158: p. 574-590.

37. Djeunou, E.D.N., et al., *Pozzolanic activities of some pyroclastic materials of Tombel Graben (Cameroon Volcanic Line) and potentiality for their use in construction industry.* Arabian Journal of Geosciences, 2021. 14(17): p. 1792.

38. Celik, K., et al., *Effect of volcanic ash pozzolan or limestone replacement on hydration of Portland cement.* Construction and Building Materials, 2019. 197: p. 803-812.

39. Nehdi, M.L. and A. Yassine, *Mitigating Portland cement CO2 emissions using alkali-activated materials: system dynamics model.* Materials, 2020. 13(20): p. 4685.

40. Robayo-Salazar, R.A., M. de Gutiérrez, and F. Puertas, *Study of synergy between a natural volcanic pozzolan and a granulated blast furnace slag in the production of geopolymeric pastes and mortars.* Construction and Building Materials, 2017. 157: p. 151-160.

41. Robayo-Salazar, R.A. and R. Mejía de Gutiérrez, *Natural volcanic pozzolans as an available raw material for alkali-activated materials in the foreseeable future: A review.* Construction and Building Materials, 2018. 189: p. 109-118.

42. Derakhshani, A., A. Ghadi, and S.E. Vahdat, *Study of the effect of calcium nitrate, calcium formate, triethanolamine, and triisopropanolamine on compressive strength of Portland-pozzolana cement.* Case Studies in Construction Materials, 2023. 18: p. e01799.

43. Lemougna, P.N., et al., *Review on the use of volcanic ashes for engineering applications.* Resources, Conservation and Recycling, 2018. 137: p. 177-190.

44. Siddique, R., *Properties of concrete made with volcanic ash.* Resources, Conservation and Recycling, 2012. 66: p. 40-44.

45. Siddique, R., *Effect of volcanic ash on the properties of cement paste and mortar.* Resources, Conservation and Recycling, 2011. 56(1): p. 66-70.

46. Hossain, K.M.A., *Chloride induced corrosion of reinforcement in volcanic ash and pumice based blended concrete.* Cement and Concrete Composites, 2005. 27(3): p. 381-390.

47. Djon Li Ndjock, B.I., A. Elimbi, and M. Cyr, *Rational utilization of volcanic ashes based on factors affecting their alkaline activation.* Journal of Non-Crystalline Solids, 2017. 463: p. 31-39.

48. Kupwade-Patil, K., et al., *Particle Size Effect of Volcanic Ash towards Developing Engineered Portland Cements.* Journal of Materials in Civil Engineering, 2018. 30(8).

49. Kupwade-Patil, K., et al., *Water dynamics in cement paste at early age prepared with pozzolanic volcanic ash and Ordinary Portland Cement using quasielastic neutron scattering.* Cement and Concrete Research, 2016. 86: p. 55-62.

50. Ghafoori, N., M. Najimi, and B. Radke, *Natural Pozzolan-based geopolymers for sustainable construction.* Environmental Earth Sciences, 2016. 75: p. 1-16.

51. Takeda, H., et al., *Fabrication and characterization of hardened bodies from Japanese volcanic ash using geopolymerization.* Ceramics International, 2014. 40(3): p. 4071-4076.

52. Kupwade-Patil, K., et al., *Particle size effect of volcanic ash towards developing engineered Portland cements.* Journal of Materials in Civil Engineering, 2018. 30(8): p. 04018190.

53. Moropoulou, A., A. Bakolas, and E. Aggelakopoulou, *Evaluation of pozzolanic activity of natural and artificial pozzolans by thermal analysis.* Thermochimica Acta, 2004. 420(1-2): p. 135-140.

54. Kupwade-Patil, K., et al., *Microstructure of cement paste with natural pozzolanic volcanic ash and Portland cement at different stages of curing.* Construction and Building Materials, 2016. 113: p. 423-441.

55. Alqarni, A.S., *A comprehensive review on properties of sustainable concrete using volcanic pumice powder ash as a supplementary cementitious material.* Construction and Building Materials, 2022. 323.

56. Martin-Rodriguez, P., et al., *Valorisation of "La Palma" Volcanic Ash for Making Portland-Blended, Alkaline and Hybrid Portland-Alkaline Cements.* Materials (Basel), 2024. 17(1).

57. Contrafatto, L., *Recycled Etna volcanic ash for cement, mortar and concrete manufacturing.* Construction and Building Materials, 2017. 151: p. 704-713.

58. Al-Bahar, S., et al., *Effect of Volcanic Ash Incorporation on the Mechanical Properties and Surface Morphology of Hydrated Cement Paste.* Journal of Materials in Civil Engineering, 2017. 29(8).

59. Belaidi, A., et al., *Effect of natural pozzolana and marble powder on the properties of self-compacting concrete.* Construction and Building Materials, 2012. 31: p. 251-257.

60. Liu, J.-C., et al., *High-performance green concrete with high-volume natural pozzolan: Mechanical, carbon emission and cost analysis.* Journal of Building Engineering, 2023. 68: p. 106087.

61. Balog, A.-A., et al., *Valorification of volcanic tuff in constructions and materials manufacturing industry.* Procedia Technology, 2014. 12: p. 323-328.

62. Bidjocka, C., et al., *Etude et évaluation de l'activité pouzzolanique des pouzzolanes de Djoungo (Cameroun).* Annales de la Faculté des Sciences de l'Université de Yaoundé, 1993: p. 133-145.

63. Kretova, V., et al., *Gypsumcementpozzolana composites with application volcanic ash.* Procedia Engineering, 2015. 117: p. 206-210.

64. Hossain, K.M.A. and M. Lachemi, *Strength, durability and micro-structural aspects of high performance volcanic ash concrete.* Cement and Concrete Research, 2007. 37(5): p. 759-766.

65. Husain, A., et al., *In situ electrochemical impedance characterization of cement paste with volcanic ash to examine early stage of hydration.* Construction and Building Materials, 2017. 133: p. 107-117.

66. Burgos, D.M., et al., *Chloride ion resistance of self-compacting concretes incorporating volcanic materials.* Construction and Building Materials, 2017. 156: p. 565-573.

67. Hossain, K.M.A. and M. Lachemi, *Performance of volcanic ash and pumice based blended cement concrete in mixed sulfate environment.* Cement and Concrete Research, 2006. 36(6): p. 1123-1133.

68. Hossain, K.M.A. and M. Lachemi, *Corrosion resistance and chloride diffusivity of volcanic ash blended cement mortar.* Cement and Concrete Research, 2004. 34(4): p. 695-702.

69. Hossain, K. and M. Lachemi, *Fresh, mechanical, and durability characteristics of self-consolidating concrete incorporating volcanic ash.* Journal of Materials in Civil Engineering, 2010. 22(7): p. 651-657.

70. Celik, K., et al., *High-volume natural volcanic pozzolan and limestone powder as partial replacements for portland cement in self-compacting and sustainable concrete.* Cement and Concrete Composites, 2014. 45: p. 136-147.

71. Martín-Rodríguez, P., et al., *Valorisation of "La Palma" Volcanic Ash for Making Portland-Blended, Alkaline and Hybrid Portland–Alkaline Cements.* Materials, 2024. 17(1): p. 242.

72. Tchakoute, H.K., et al., *Synthesis of geopolymers from volcanic ash via the alkaline fusion method: Effect of Al2O3/Na2O molar ratio of soda–volcanic ash.* Ceramics International, 2013. 39(1): p. 269-276.

73. Djobo, J.N.Y., et al., *Volcanic ash-based geopolymer cements/concretes: the current state of the art and perspectives.* Environmental Science and Pollution Research, 2017. 24: p. 4433-4446.

74. Alraddadi, S., *Effects of calcination on structural properties and surface morphology of black volcanic ash.* Journal of Physics Communications, 2020. 4(10): p. 105002.

75. Patel, R., F. Kinney, and G. Schumacher. *Green concrete using 100% fly ash based hydraulic binder*. in *Int. Concr. Sustain. Conf*. 2012.

76. Robayo-Salazar, R.A., R.M. De Gutiérrez, and F. Puertas, *Effect of metakaolin on natural volcanic pozzolan-based geopolymer cement.* Applied Clay Science, 2016. 132: p. 491-497.

77. Kouamo, H.T., et al., *Synthesis of volcanic ash-based geopolymer mortars by fusion method: Effects of adding metakaolin to fused volcanic ash.* Ceramics International, 2013. 39(2): p. 1613-1621.

78. Hossain, K., *Properties of volcanic ash and pumice concrete.* IABSE Report, 1999. 80: p. 145-150.

79. Provis, J.L., *Alkali-activated materials.* Cement and Concrete Research, 2018. 114: p. 40-48.

80. Bondar, D., et al., *Effect of adding mineral additives to alkali-activated natural pozzolan paste.* Construction and Building Materials, 2011. 25(6): p. 2906-2910.

81. Robayo-Salazar, R., et al., *Alkali-activated binary mortar based on natural volcanic pozzolan for repair applications.* Journal of Building Engineering, 2019. 25: p. 100785.

82. Khan, K., et al., *Effect of fineness of basaltic volcanic ash on pozzolanic reactivity, ASR expansion and drying shrinkage of blended cement mortars.* Materials, 2019. 12(16): p. 2603.

83. Anwar Hossain, K.M., *Lightweight concrete incorporating volcanic materials.* Proceedings of the Institution of Civil Engineers-Construction Materials, 2012. 165(2): p. 111-120.

84. Bawab, J., et al., *Effect of different activation techniques on the engineering properties of cement-free binder containing volcanic ash and calcium carbide residue.* Construction and Building Materials, 2023. 408: p. 133734.

85. Lemougna, P.N., K.J.D. MacKenzie, and U.F.C. Melo, *Synthesis and thermal properties of inorganic polymers (geopolymers) for structural and refractory applications from volcanic ash.* Ceramics International, 2011. **37**(8): p. 3011-3018.

86. Contrafatto, L., et al., *Physical, mechanical and thermal properties of lightweight insulating mortar with recycled Etna volcanic aggregates.* Construction and Building Materials, 2020. **240**: p. 117917.

87. Hossain, K.M.A., *Blended cement using volcanic ash and pumice.* Cement and Concrete Research, 2003. **33**(10): p. 1601-1605.

88. Olawuyi, B. and K.O. Olusola, *Compressive strength of volcanic ash/ordinary portland cement laterized concrete.* Civil Engineering Dimension, 2010. **12**(1): p. 23-28.

89. Briggs, R.M., *Geology Of Tauranga Area.* 1996.

90. Theophanides, T., *Infrared Spectroscopy-Materials Science, Engineering and Technology*. 2012, InTech.

91. Aydin, A.C. and R. Gül, *Influence of volcanic originated natural materials as additives on the setting time and some mechanical properties of concrete.* Construction and Building Materials, 2007. **21**(6): p. 1277-1281.

92. Al-Bahar, S., et al., *Effect of volcanic ash incorporation on the mechanical properties and surface morphology of hydrated cement paste.* Journal of Materials in Civil Engineering, 2017. **29**(8): p. 04017052.

93. Jumate, E. and D.L. Manea, *Application of X-ray diffraction (XRD) and scanning electron microscopy (SEM) methods to the portland cement hydration processes.* J. Appl. Eng. Sci, 2012. **2**(1): p. 35-42.

94. Provis, J.L., et al., *X-ray microtomography shows pore structure and tortuosity in alkali-activated binders.* Cement and concrete research, 2012. **42**(6): p. 855-864.

95. Lloyd, R.R., J.L. Provis, and J.S.J. van Deventer, *Microscopy and microanalysis of inorganic polymer cements. 1: remnant fly ash particles.* Journal of Materials Science, 2009. **44**(2): p. 608-619.

96. Elsalamawy, M., A.R. Mohamed, and A.-l.E. Abosen, *Performance of crystalline forming additive materials in concrete.* Construction and Building Materials, 2020. **230**: p. 117056.

97. Kriskova, L., et al., *Hydraulic behavior of mechanically and chemically activated synthetic merwinite.* Journal of the American Ceramic Society, 2014. **97**(12): p. 3973-3981.

98. Shi, L.-S., L.-Y. Wang, and Y.-N. Wang, *The investigation of argon plasma surface modification to polyethylene: Quantitative ATR-FTIR spectroscopic analysis.* European Polymer Journal, 2006. **42**(7): p. 1625-1633.

99. Yusuf, M.O., *Bond Characterization in Cementitious Material Binders Using Fourier-Transform Infrared Spectroscopy.* Applied Sciences, 2023. **13**(5): p. 3353.

100. University, K.P., *IR Spectrum and Characteristic Absorption Bands.* 2021.

101. Saleh, M., et al., *Malachite Green Dye Removal from Aqueous Solutions Using Invader Centaurea Solstitialis Plant and Optimization by Response Surface Method: Kinetic, Isotherm, And Thermodynamic Study.* Avrupa Bilim ve Teknoloji Dergisi, 2019(17): p. 755-768.

102. Prodjosantoso, A.K., et al. *The Use of Saccharum Officinarum Bagasse and Chicken Eggshells to Synthesize Calcium Silicates*. in *9th International Conference on Education Research, and Innovation (ICERI 2021)*. 2022. Atlantis Press.

103. Fatima, S., et al., *Facile Synthesis of Sodium Alginate (SA)-Based Quaternary Bio-Nanocomposite (SA@Co-Zn-Ce) for Antioxidant Activity and Photocatalytic Degradation of Reactive Red 24.* Catalysts, 2024. **14**(8): p. 471.

104. Yu, P., et al., *Structure of calcium silicate hydrate (C-S-H): Near-, Mid-, and Far-infrared spectroscopy.* Journal of the American Ceramic Society, 1999. **82**(3): p. 742-748.

105. Puertas, F. and A. Fernández-Jiménez, *Mineralogical and microstructural characterisation of alkali-activated fly ash/slag pastes.* Cement and Concrete composites, 2003. **25**(3): p. 287-292.

106. Robayo-Salazar, R.A., R. Mejía de Gutiérrez, and F. Puertas, *Effect of metakaolin on natural volcanic pozzolan-based geopolymer cement.* Applied Clay Science, 2016. **132-133**: p. 491-497.

107. Guan, W., et al., *Synthesis and enhanced phosphate recovery property of porous calcium silicate hydrate using polyethyleneglycol as pore-generation agent.* Materials, 2013. **6**(7): p. 2846-2861.

108. Lopez-Salas, J. and J.I. Escalante-Garcia, *Hybrid binders based on volcanic pumice: Effect of the chemical composition on strength and microstructures.* Cement and Concrete Research, 2024. **176**: p. 107393.

109. Jativa, A. and M. Etxeberria, *Exploring the Utilization of Activated Volcanic Ash as a Substitute for Portland Cement in Mortar Formulation: A Thorough Experimental Investigation.* Materials (Basel), 2024. **17**(5).

110. El-Jazairi, B. and J. Illston, *A simultaneous semi-isothermal method of thermogravimetry and derivative thermogravimetry, and its application to cement pastes.* Cement and Concrete Research, 1977. **7**(3): p. 247-257.

111. Vedalakshmi, R., et al., *Quantification of hydrated cement products of blended cements in low and medium strength concrete using TG and DTA technique.* Thermochimica Acta, 2003. **407**(1-2): p. 49-60.

112. Monteagudo, S., et al., *The degree of hydration assessment of blended cement pastes by differential thermal and thermogravimetric analysis. Morphological evolution of the solid phases.* Thermochimica Acta, 2014. **592**: p. 37-51.

113. Bhatty, J.I., *Hydration versus strength in a portland cement developed from domestic mineral wastes — a comparative study.* Thermochimica Acta, 1986. **106**: p. 93-103.